Combating Biofilms and Antibiotic Resistance using Synthetic Biology

by

Timothy Kuan-Ta Lu

S.B. Electrical Engineering and Computer Science
M.Eng. Electrical Engineering and Computer Science
Massachusetts Institute of Technology, 2003

SUBMITTED TO THE HARVARD-MIT DIVISION OF HEALTH SCIENCES AND TECHNOLOGY IN PARTIAL FULFILLMENT OF THE REQUIREMENTS FOR THE DEGREE OF

DOCTOR OF PHILOSOPHY IN ELECTRICAL AND BIOMEDICAL ENGINEERING
AT THE
MASSACHUSETTS INSTITUTE OF TECHNOLOGY

FEBRUARY 2008

Signature of Author: _____
Harvard-MIT Division of Health Sciences and Technology
December 12, 2007

Certified by: _____
James J. Collins, Ph.D.
Professor of Biomedical Engineering
Boston University
Thesis Supervisor

Accepted by: _____
Martha L. Gray, Ph.D.
Edward Hood Taplin Professor of Medical and Electrical Engineering
Director, Harvard-MIT Division of Health Sciences and Technology

Combating Biofilms and Antibiotic Resistance using Synthetic Biology

by

Timothy Kuan-Ta Lu

Submitted to the Harvard-MIT Division of Health Sciences and Technology
on December 12, 2007 in Partial Fulfillment of the
Requirements for the Degree of Doctor of Philosophy in
Electrical and Biomedical Engineering.

ABSTRACT

Bacterial infections represent a significant source of morbidity and mortality. Biofilms and antibiotic resistance pose challenges to our future ability to treat bacterial diseases with antibiotics (1). Bacteria frequently live in biofilms, which are surface-associated communities encased in a hydrated extracellular polymeric substances (EPS) matrix (2, 3). Biofilms are crucial in the pathogenesis of many clinically-important infections and are difficult to eradicate because they exhibit resistance to antimicrobial agents and removal by host immune systems (4). Antibiotics can even induce biofilm formation (5, 6).

The development of antibiotic-resistant bacteria is also a growing medical problem. Antibiotic-resistance genes can be acquired by horizontal gene transfer and passed vertically to later generations (7). Antibiotic resistance can also result from persistence, a phenomena in which a subpopulation of cells can withstand antibiotic treatment without containing antibiotic-resistance genes (8). These problems, coupled with decreasing output of new antibiotics, have highlighted the need for new treatments for bacterial infections (1, 9-12).

I developed three novel strategies for attacking bacterial biofilms and antibiotic resistance using synthetic biology. To remove biofilms, I engineered bacteriophage to express a biofilm-degrading enzyme during infection to simultaneously attack biofilm cells and the biofilm EPS matrix. These enzymatically-active bacteriophage substantially reduced biofilm cell counts by 4.5 orders of magnitude (~99.997% removal), which was about two orders of magnitude better than that of non-enzymatic phage. To address antibiotic-resistant bacteria, I targeted gene networks with synthetic bacteriophage to create antibiotic adjuvants. Suppressing the SOS network with engineered bacteriophage enhanced killing by ofloxacin, a quinolone drug, by over 2.7 and 4.5 orders of magnitude compared with control bacteriophage plus ofloxacin and ofloxacin alone, respectively. I also built phage that targeted multiple gene networks and demonstrated their effectiveness as antibiotic adjuvants. Engineered bacteriophage reduced the number of antibiotic-resistant bacteria and performed as strong adjuvants for other bactericidal antibiotics such as aminoglycosides and β-lactams. Finally, I designed synthetic *in vivo* sensors for antibiotic-resistance genes that can be coupled with effector components to kill cells carrying resistance genes or to block horizontal transmission of those genes. My work demonstrates the

feasibility and benefits of using engineered bacteriophage and synthetic biology constructs to address the dual threats of bacterial biofilms and antibiotic-resistant bacteria.

Thesis Supervisor: James Collins
Title: Professor of Biomedical Engineering, Boston University

ACKNOWLEDGEMENTS

The process of obtaining a Ph.D. is long and tough, albeit a rewarding one. I am very appreciative for the support and encouragement of my family and many close friends. My parents, Nicky and Sue, have been supportive of my education through my entire life and for that I am ever grateful. I would like to thank Sandy, my significant other, for her understanding, encouragement, and humor throughout my Ph.D. education and for sustaining me as I complete my future medical degree. My family members, including my brother Jeff, my cousins, my aunts and uncles, and my grandparents, have been instrumental in keeping my spirits high while pursuing a higher education. Thank you so much.

I've had the good fortune and pleasure of being mentored by many great minds, including, but certainly not limited to, Prof. James Collins, Prof. Collin Stultz, Prof. Rahul Sarpeshkar, Prof. George Church, Prof. Gregory Stephanopoulos, Prof. Thomas Rocco, Prof. Joel Katz, Prof. Brian Hoffman, Prof. Peter Dallos, and Prof. James Meindl. Prof. James Collins has been generous to give me financial and intellectual support throughout my Ph.D. Special thanks to my thesis committee, composed of Prof. James Collins, Prof. George Church, and Prof. Gregory Stephanopoulos for their time and effort. I especially appreciate the support and guidance of Prof. Collin Stultz with regards to my pursuit of an M.D. I greatly appreciate the intellectual conversations I've had with Ali Shoeb, David Nguyen, Dan Dwyer, Michael Koeris, Michael Kohanski, Lakshminarayan Srinivasan, Philip Lee, and many other colleagues and friends. I am extremely grateful for my close friends who have always kept me in good spirits despite being dispersed all over the globe and busy with their own exciting careers.

I am appreciative of comments on my work from Prof. James Collins, Nicholas Guido, Dan Dwyer, Philina Lee, Michael Koeris, Michael Kohanski, Ari Friedland, and other members of the Collins Lab and the Sarpeshkar Lab. My research has been supported by the Department of Energy and the National Science Foundation. I have also been fortunate to be funded by a Howard Hughes Medical Institute Predoctoral Fellowship and a Harvard/MIT Health Sciences and Technology Medical Engineering/Medical Physics Fellowship.

BIOGRAPHY

I was born in California and grew up in Yorktown Heights, New York until 1990, at which point I moved back to Taiwan. After completing middle school at the National Experimental High School Bilingual Department in Hsinchu, Taiwan, I attended high school at Taipei American School. I graduated valedictorian in 1999 and entered MIT as a freshman. As an undergraduate, I worked at an MIT software startup company named EyeShake Inc., the Tangible Media Group in the MIT Media Lab, Project WF at the IBM Almaden Research Center, and the Analog VLSI and Biological Systems Group in the MIT Research Laboratory of Electronics. At the same time, I obtained my S.B. and M.Eng. degrees in Electrical Engineering and Computer Science (1999-2003). I also received Minors in Biology and Biomedical Engineering and a Concentration in Economics. My M.Eng. thesis was entitled "*A Feedback Analysis of Outer Hair Cell Dynamics*" and provided a solution for a twenty-year-old open question in cochlear mechanics which asked how low-frequency outer hair cells operate as high-frequency amplifiers in the cochlea.

Subsequently, I entered the Harvard/MIT Health Sciences and Technology Medical Engineering/Medical Physics (HST MEMP) Ph.D. program. Thanks to the flexibility of the HST MEMP program, I was free to explore research in any respected laboratory in the Boston area. I joined the laboratory of Prof. James Collins at Boston University and spent 4.5 years completing my Ph.D. program. I was able to pursue this unusual and fruitful arrangement with the generous support of the Howard Hughes Medical Institute Predoctoral Fellowship. My work has been published in journals such as the *Proceedings of the National Academy of Sciences* and featured in diverse publications, including *Nature*, *PLoS Biology*, *Technology Review*, and MSNBC.

During my graduate career, I continued working on entrepreneurial projects outside of my doctoral research. I was a team member of Asymmetrix, a 2004 MIT $50K Entrepreneurship Competition Semifinalist focused on mass-producing human red blood cells for transfusions. I produced business research for Asymmetrix and delivered the business pitch at the Competition's Semifinalist presentation. I also worked with CellASIC Corporation, a leading-edge microfluidics startup company, to develop automation software and hardware for proprietary microfluidic devices for laboratory and industrial applications. In addition, I am a founder and partner at Womper Inc., a technology-based startup company focused on producing useful and stimulating Internet applications.

In addition to working on doctoral research and entrepreneurial activities, I enrolled in preclinical courses at Harvard Medical School. I took these classes while I was conducting Ph.D. research and the two activities complemented each other rather well on an intellectual level. After participating in the Introduction to Clinical Medicine courses at the West Roxbury Veterans Hospital, I decided to pursue my M.D. after my Ph.D. and have applied for transfer into the Harvard M.D. program. I wish to dedicate my career to the translation of basic biomedical research to clinical practice in academic, medical, and entrepreneurial settings. Finally, any short biography of mine would be incomplete if I did not include one of the happiest events of my life, my engagement to my sweetheart, Sandy, in the winter of 2007-2008.

Journal Papers

T. K. Lu and J. J. Collins, "Engineered Bacteriophage Targeting Non-essential Gene Networks as Adjuvants for Antibiotic Therapy," *submitted*, 2007.

T. K. Lu and J. Collins, "Dispersing Biofilms with Engineered Enzymatic Bacteriophage," *Proceedings of the National Academy of Science*, vol. 104, no. 27, pp. 11197-11202, July 3, 2007. (http://www.pnas.org/cgi/content/abstract/0704624104v1). In the top 15 most read articles in July 2007.

T. K. Lu, S. Zhak, P. Dallos, and R. Sarpeshkar, "Fast cochlear amplification with slow outer hair cells," *Hearing Research*, vol. 214, no. 1-2, pp. 45-67, April 2006. (http://dx.doi.org/10.1016/j.heares.2006.01.018)

R. Sarpeshkar, C. Salthouse, J.-J. Sit, M. Baker, S. Zhak, **T. K.-T. Lu**, L. Turicchia, and S. Balster, "An Ultra-Low-Power Programmable Analog Bionic Ear Processor," *IEEE Transactions on Biomedical Engineering*, vol. 52, no. 4, pp. 711-727, April 2005. (http://dx.doi.org/10.1109/TBME.2005.844043)

Peer-Reviewed Conference Papers

T. K. Lu, S. Zhak, P. Dallos, and R. Sarpeshkar, "A Micromechanical Model for Fast Cochlear Amplification with Slow Outer Hair Cells", *Proceedings of the International Symposium on Auditory Mechanisms: Processes and Models*, pp. 433-441, Portland, Oregon, July 23-28, 2005.

M.W. Baker, **T. K.-T. Lu**, and R. Sarpeshkar, "A Low-Power AGC with Level Independent Phase Margin," *IEEE 2004 American Controls Conference*, Boston, MA, vol. 1, pp. 386-389, June 30-July 2, 2004.

M.W. Baker, **T. K.-T. Lu**, C.D. Salthouse, J.-J. Sit, S. Zhak, and R. Sarpeshkar, "A 16-channel Analog VLSI Processor for Bionic Ears and Speech-Recognition Front Ends," invited paper, *Proceedings of the IEEE Custom Integrated Circuits Conference*, San Jose, CA, vol. 23, no. 4, pp. 521-526, Sep. 21-24, 2003. (http://dx.doi.org/10.1109/CICC.2003.1249452)

T. K.-T. Lu, M. Baker, C. Salthouse, J.-J. Sit, S. Zhak, and R. Sarpeshkar, "A Micropower Analog VLSI Processing Channel for Bionic Ears and Speech-Recognition Front Ends," *Proceedings of the 2003 IEEE International Symposium on Circuits and Systems (ISCAS 03)*, Bangkok, Thailand, vol. 5, pp. 41-44, May 25-28, 2003. (http://dx.doi.org/10.1109/ISCAS.2003.1206169)

Technical Reports

T. K. Lu, S. Zhak, P. Dallos, and R. Sarpeshkar, "Fast Cochlear Amplification with Slow Outer Hair Cells," *Massachusetts Institute of Technology Microsystems Technology Laboratories Annual Research Report*, pp. 40, September, 2006.

Honors & Awards

- Howard Hughes Medical Institute (HHMI) Predoctoral Fellowship in Biological Sciences (2003)
- Harvard/MIT Health Sciences & Technology Medical Engineering/Medical Physics Graduate Fellowship (2003)
- Siebel Scholar Award (2003), *$25,000 Graduate Fellowship*
- Johnson & Johnson Biomedical Engineering Research Prize (2003)
- National Science Foundation Graduate Fellowship (2003), *declined in favor of HHMI fellowship*
- National Defense Science and Engineering Graduate Fellowship (2003), *declined in favor of HHMI fellowship*
- Whitaker Foundation Graduate Fellowship in Biomedical Engineering (2003), *declined in favor of HHMI fellowship*
- Caltech Engineering and Applied Sciences Fellowship (2003), *declined in favor of Harvard/MIT HST Program*
- Stanford Graduate Fellowship (2003), *declined in favor of Harvard/MIT HST Program*
- UC Berkeley Fellowship for Graduate Study (2003), *declined in favor of Harvard/MIT HST Program*
- UC Berkeley Bioengineering Craven Fellowship (2003), *declined in favor of Harvard/MIT HST Program*
- UC Berkeley $2000 Graduate Bonus for NSF Fellowship (2003), *declined in favor of Harvard/MIT HST Program*
- UC San Diego $2000 Graduate Bonus for NSF Fellowship (2003), *declined in favor of Harvard/MIT HST Program*
- Hertz Foundation Graduate Fellowship Finalist (2003)
- Bioengineering Undergraduate Research Award (2002)
- Winner of Analog Circuits Laboratory Project Award (2002)
- U.S. National Merit Scholar (1999)
- Sigma Xi Scientific Research Society
- Tau Beta Pi
- Eta Kappa Nu
- National Society of Collegiate Scholars

TABLE OF CONTENTS

LIST OF TABLES

LIST OF FIGURES

1 INTRODUCTION

Biofilms and antibiotic resistance pose a significant hurdle to eliminating bacterial infections with conventional antimicrobial drugs. Patients that would have been easily cured by antibiotics in the past are now dying or remaining sick for much longer due to biofilms and antibiotic-resistant bacterial infections (10, 13, 14). The economic cost of antibiotic resistance in the United States alone is estimated to be between US $5 billion and US $24 billion per year (15). Therefore, it is imperative that new antibacterial strategies be explored (16).

Bacteria frequently live in biofilms, which are surface-associated communities enclosed in a hydrated extracellular polymeric substances (EPS) matrix composed of polysaccharides, proteins, nucleic acids, and lipids which helps maintain a complex heterogeneous structure (2, 3). Biofilms constitute an essential and protective lifestyle for bacteria in many different natural and man-made environments, including dental plaques, water pipes, medical devices, and industrial systems (17). Bacterial biofilms have been implicated as a source of persistent infection, contamination, and biofouling due to inherent resistance to antimicrobial agents and host immune defenses (18). Thus, there exists a growing need for novel and effective treatments targeted at biofilms, particularly in light of the continually-worsening problem of antibiotic resistance and the discovery that antibiotic use can even induce biofilm formation (5, 6).

In addition to inherent bacterial resistance to antimicrobials in biofilm, antibiotic resistance can result from mutations in antibacterial targets or from acquisition of genes that encode proteins which promote the efflux of antibiotics or bind and inactivate antibiotics (7). Gene acquisition is usually due to horizontal gene transfer via transformation, plasmids, or conjugative transposons (19, 20). For example, *Enterococcus faecalis* in nosocomial settings became

completely vancomycin-resistant by 1988 (19). Co-infecting staphylococci have subsequently received *vanA* resistance genes from *Enterococcus faecalis* (19). *Staphylococcus aureus* acquired resistance to sulpha drugs in the 1940s, penicillin-resistance in the 1950s, methicillin-resistance in the 1980s, and vancomycin-resistance in 2002 (19). The heavy use of antibiotics in livestock in the agricultural industry has contributed to the emergence of methicillin-resistant staphylococci and is unlikely to abate (19). *Streptococcus pneumoniae* and *Neisseria gonorrhoeae* have also obtained resistance to antibiotics (19).

Another way for bacterial cells to be resistant to antimicrobial agents is through the phenomena of persistence (8). Persistence is believed to be a stochastic process in which certain cells in a metabolically-dormant stage are able to avoid being killed by multiple antibiotics (8). Persisters do not carry genetic mutations but instead exhibit phenotypic resistance to antibiotics (21). In *E. coli*, persister levels increase markedly in late-exponential and stationary phases and are important components of biofilm (8). Chromosomally-encoded toxins may contribute to the persister phenotype (22-24). However, the underlying mechanisms controlling the stochastic process of persistence are not well understood (8).

Proposed solutions to limit the spread of antibiotic resistance include reducing antibiotic use, preventing the spread of resistant bacteria particularly in nosocomial settings, using novel antibiotics to which pathogens are not resistant, and limiting person-to-person transmission by reducing the carrier rate in health-care workers and patients (10). These attempts to control the spread of antibiotic resistance require great design, compliance, and effort to achieve efficacy. While these techniques may certainly help control the spread of antibiotic resistance, they may be difficult to implement successfully in real life and cannot avoid the evolutionary pressure that antibiotic use places on bacteria to select for resistance. For example, ecological models of

antibiotic cycling suggest that conventional cycling will not reduce antimicrobial resistance in hospitals (25). In many cases, bacteria with antibiotic resistance genes maintain them stably and do not fare poorly against non-resistant strains (8). Constant evolutionary pressure will ensure that antibiotic resistance bacteria will continue to grow in number. The dearth of new antibacterial agents being developed in the last 25-30 years certainly bodes poorly for the future of the antibiotic era (1). Thus, new methods for combating bacterial infections are needed in order to prolong the antibiotic age. For example, bacteriophage therapy or synthetic antibacterial peptides have been proposed as potential solutions (16, 26).

Phage therapy has begun to be accepted in industrial and biotechnological settings. For example, the FDA recently approved the use of phage targeted at *Listeria monocytogenes* as a food additive (27). However, phage therapy has several challenges that must be overcome before it will be accepted in Western medicine for treating humans (28). These problems include the lack of properly designed clinical trials to date (28), development of phage resistance (11, 12, 29), phage immunogenicity in the human body and clearance by the reticuloendothelial system (RES) (11, 30), the release of toxins upon bacterial lysis (11), and phage specificity (11). Fortunately, many of these concerns are currently being studied and addressed. For example, combination therapy with antibiotics and phage may alleviate the development of phage resistance (11, 12, 29). Long-circulating phage can be isolated that can avoid RES clearance to increase *in vivo* efficacy (30). The problem of phage clearance is an important one that needs to be solved as it may make phage therapy more useful for treating transient infections rather than chronic ones. Non-lytic and non-replicative phage have been engineered to kill bacteria while minimizing endotoxin release (31, 32). Progress is also being made in the development of toxin-free phage preparations (33).

The specificity of phage for host bacteria is both an advantage and a disadvantage for phage therapy. Specificity allows human cells as well as innocuous bacteria to be spared, potentially avoiding serious issues such as drug toxicity or *Clostridium difficile* overgrowth that can arise with antibiotic use. *C. difficile* infection is characterized by diarrhea and colitis, and has increased in severity in recent years (34). Antibiotic therapy is believed to alter the microbial flora in the colon due to lack of target specificity, thus allowing *C. difficile* to proliferate and cause disease (35). However, host specificity means that a well-characterized library of phage must be maintained so that an appropriate therapy can be designed for each individual infection (11). The diversity of bacterial infections implies that it may be difficult for any particular engineered phage to be a therapeutic solution for a wide range of biofilms. Indeed, phage therapy generally requires the use of phage cocktails to cover a range of target bacteria.

To reduce biofilms, I have developed an enzymatically-active bacteriophage platform to produce phage which express biofilm-dispersing enzymes during infection followed by cell lysis. To attack antibiotic-resistant bacteria, I built a synthetic bacteriophage platform to target gene networks as antibiotic adjuvants. Finally, I developed synthetic *in vivo* sensors to detect the presence of antibiotic-resistant genes within individual bacterial cells. These sensors can be connected to downstream synthetic effector components which kill bacteria that carry resistance genes or suppress horizontal transmission of those genes. These are synthetic biology solutions for the important dual threats of biofilms and antibiotic-resistant bacteria.

2 ENGINEERED PHAGE THERAPY FOR BACTERIAL BIOFILMS

2.1 Introduction

Over the last few years, synthetic biology has enabled the development of many engineered biological devices and cells with interesting and well-modelled characteristics (36-38). At the same time, new technologies for more cost-effective DNA synthesis and sequencing have been reported (39). These advances allow for large-scale synthetic genomes to be designed and built with much greater ease than is currently possible with traditional molecular biology methods. Synthetic biologists have begun to address important real-world problems by modifying organisms to produce artemisin precursors (40), developing bacteria that can target cancerous cells (41), and producing new antimicrobial peptides (16), to name a few examples (37). Synthetic biology is distinguished from traditional genetic engineering through the use of modularity, abstraction, and standardization to allow generalized principles and designs to be applied to different scenarios. In this work, I engineered bacteriophage with biofilm-degrading enzymatic activity to create a synthetic biology platform for eradicating bacterial biofilms. The text used in this section to describe this work was published and therefore reproduced from Ref. (42) in *Proceedings in the National Academy of Sciences*.

Bacteria frequently live in biofilms, which are surface-associated communities encased in a hydrated EPS matrix, that is composed of polysaccharides, proteins, nucleic acids, and lipids and helps maintain a complex heterogeneous structure (2, 3). Biofilms constitute an essential and protective lifestyle for bacteria in many different natural and man-made environments, including dental plaques, water pipes, medical devices, and industrial systems (17). Bacterial biofilms have been implicated as a source of persistent infection and contamination in medical, industrial, and

food processing settings due to inherent resistance to antimicrobial agents and host defenses (2, 4, 18, 43). Thus, there exists a growing need for novel and effective treatments targeted at biofilms, particularly in light of the continually-worsening problem of antibiotic resistance and the discovery that antibiotic use can even induce biofilm formation (5, 6).

Bacteriophage treatment has been proposed as one method for controlling bacterial biofilms (26). Phage have been used since the early 20th century to treat bacterial infections, especially in Eastern Europe, and have been shown to decrease biofilm formation (26, 28, 44). For example, phage T4 can infect and replicate within *Escherichia coli* biofilms and disrupt biofilm morphology by killing bacterial cells (45-47). Phage have also been modified to extend their natural host range. *E. coli* which produce the K1 polysaccharide capsule are normally resistant to infection by T7, but are susceptible to T7 that have been designed to express K1-5 endosialidase (48). Enzymatic degradation of EPS components is another useful strategy for disrupting biofilms, though bacterial cells are not killed, which may result in the release of many bacteria into the environment (2, 49, 50). For instance, enzymatic degradation of a cell-bound EPS polysaccharide adhesin known as polymeric β-1,6-*N*-acetyl-D-glucosamine (PGA) by exogenously-applied dispersin B (DspB) has been demonstrated to reduce biofilms of several different species of bacteria (49, 51). DspB, an enzyme which is produced by *Actinobacillus actinomycetemcomitans,* hydrolyzes PGA, a crucial adhesin needed for biofilm formation and integrity in *Staphylococcus* and *E. coli*, including *E. coli* K-12 as well as clinical isolates (51). Reports of natural lytic phage with phage-borne polysaccharide depolymerases have shown that phage-induced lysis and EPS degradation are used in combination in natural systems to reduce bacterial biofilms (52, 53). These depolymerases appear to be carried on the surfaces of phage and degrade bacterial capsular polysaccharides to allow access to bacterial cell surfaces (54).

However, the chance that one can isolate a natural phage that is both specific for the bacteria to be targeted and expresses a relevant EPS-degrading enzyme is likely to be low (11).

Therefore, I propose a modular design strategy in which phage that kill bacteria in a species-specific manner are engineered to express the most effective EPS-degrading enzymes specific to the target biofilm. This strategy should permit the development of a diverse library of biofilm-dispersing phage rather than trying to isolate such phage from the environment. By multiplying within the biofilm and hijacking the bacterial machinery, engineered enzymatically-active phage should be able to achieve high local concentrations of both enzyme and lytic phage to target multiple biofilm components, even with small initial phage inoculations. Rapid phage replication with subsequent bacterial lysis and expression of biofilm-degrading enzymes should render this two-pronged attack strategy an efficient, autocatalytic method for removing bacterial biofilms in environmental, industrial, and clinical settings (Figure 1). This design also removes the need to express, purify, and deliver large doses of enzyme to specific sites of infection that may be difficult to access, and should improve the efficacy of phage therapy at removing biofilms. Increasingly cost-effective genome sequencing and synthetic biology technologies, which include the refactoring of phage genomes and large-scale DNA synthesis (37, 55, 56), should further enable the production of engineered enzymatic phage and significantly extend the limited repertoire of biofilm-degrading phage that have been isolated from the environment.

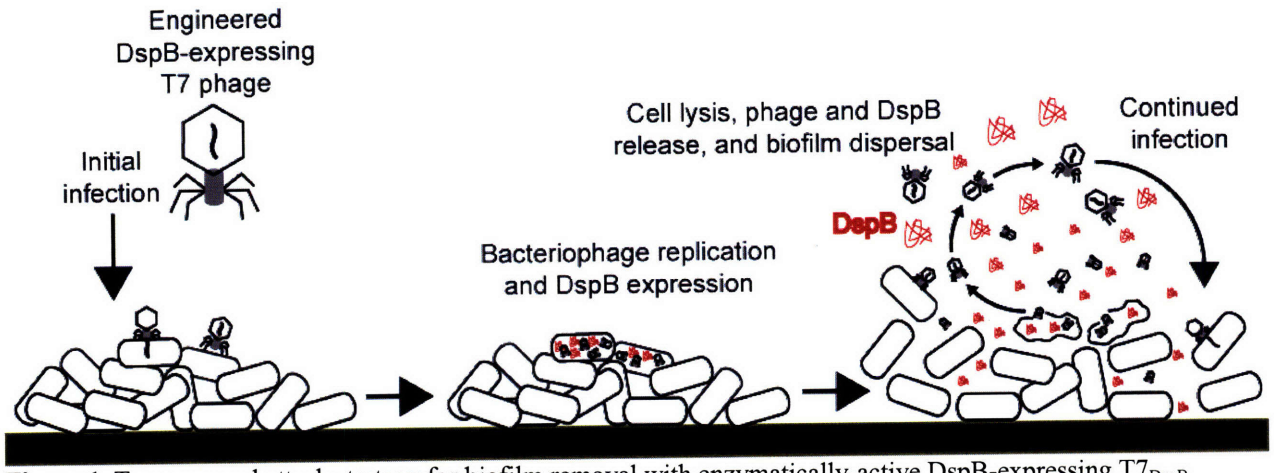

Figure 1. Two-pronged attack strategy for biofilm removal with enzymatically-active DspB-expressing $T7_{DspB}$ phage. Initial infection of *E. coli* biofilm results in rapid multiplication of phage and expression of DspB. Both phage and DspB are released upon lysis, leading to subsequent infection as well as degradation of the crucial biofilm EPS component, β-1,6-N-acetyl-D-glucosamine (49). Adapted from Ref. (42).

2.2 *Results*

2.2.1 Design of Enzymatically-Active Bacteriophage.

As a proof-of-principle design of artificial biofilm-degrading bacteriophage, I engineered T7, an E. coli-specific phage (57, 58), to express DspB intracellularly during infection so DspB would be released into the extracellular environment upon cell lysis (Figure 1). I employed a modified T7 strain (Novagen T7select415-1) with several deletions of nonessential genes (Figure 2a). I cloned the gene coding for DspB (*dspB*) under the control of the strong T7 φ10 promoter so dspB would be strongly transcribed by T7 RNA polymerase during infection (Figure 2b). As a control, I cloned an *S·Tag* insert into the T7 genome so that no DspB would be produced (Figure 2c).

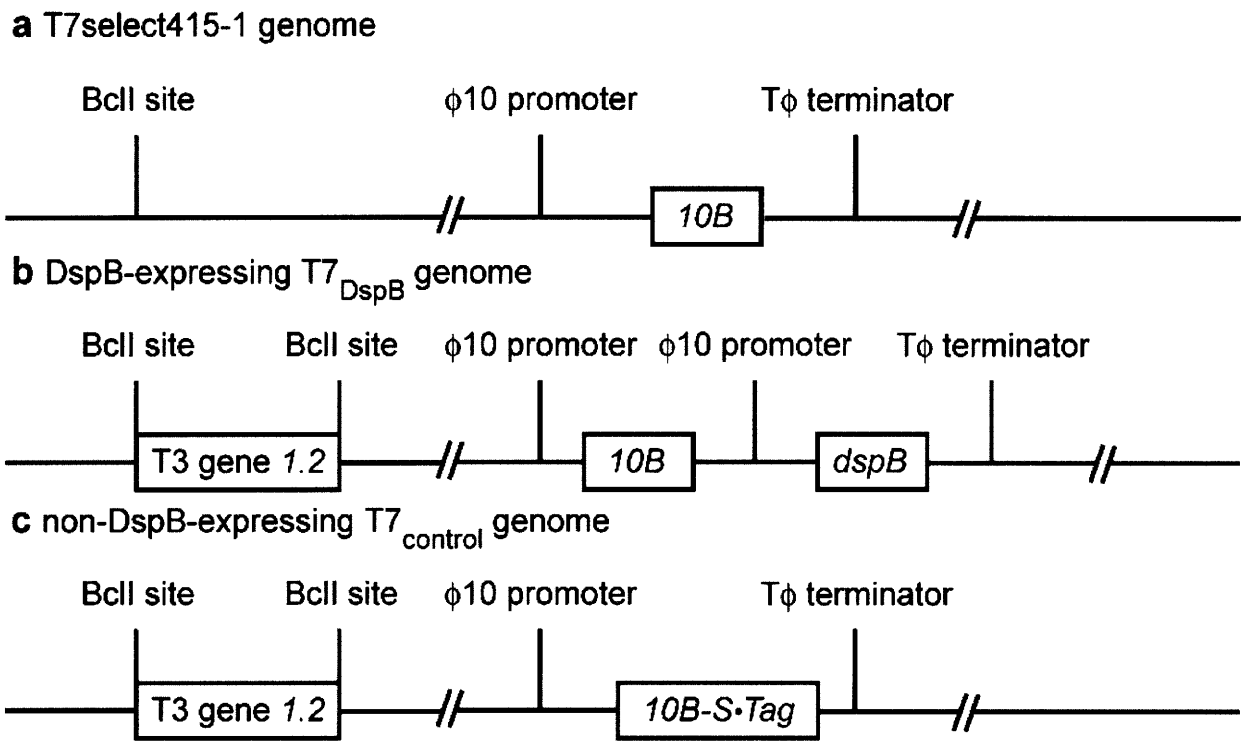

Figure 2. Genomes of engineered phage used for biofilm treatment. **(a)** Genome of T7select415-1 shows a unique BclI site and capsid gene *10B*. **(b)** DspB-expressing phage $T7_{DspB}$ was created by cloning T3 gene *1.2* into the unique BclI site and cloning the φ10-*dspB* construct after capsid gene *10B*. **(c)** Non-DspB-expressing control phage $T7_{control}$ was created by cloning T3 gene *1.2* into the unique BclI site and cloning the control *S·Tag* insert (included in the T7select415-1 kit) as a fusion with the capsid gene *10B*. Adapted from Ref. (42).

To test the effectiveness of our engineered phage against pre-grown biofilm, I cultivated *E. coli* TG1(*lacI*::*kan*) biofilms in LB media on plastic pegs using the standardized MBEC biofilm cultivation system. I used *E. coli* TG1 as the target biofilm strain since TG1 forms a thick, mature biofilm and contains the F plasmid (59). The F plasmid enhances biofilm maturation along with other biofilm-promoting factors in *E. coli*, including PGA, flagellum, cellulose, curli, antigen 43, and other conjugative pili and cell surface adhesins (59, 60). Because T7 is unable to replicate efficiently in F-plasmid-containing *E. coli*, gene *1.2* from T3 phage was also cloned into the unique BclI site in our engineered T7 phage and control T7 phage to circumvent F-plasmid-mediated exclusion and extend the phage host range (Figure 2b and Figure 2c) (61). The control phage and engineered phage were named $T7_{control}$ and $T7_{DspB}$, respectively (Figure 2b and Figure 2c).

2.2.2 Characterization of Enzymatically-Active Bacteriophage

To determine whether the $T7_{DspB}$ phage was more effective than the $T7_{control}$ phage, I first employed a crystal violet (CV) assay to assess the amount of biofilm on the pegs after phage treatment. Pre-grown TG1(*lacI*::*kan*) biofilm was inoculated with only LB media or infected with 10^3 plaque forming units per peg (PFU/peg) of $T7_{control}$ or $T7_{DspB}$ phage (Figure 3a). To assess whether our engineered enzymatic phage was more efficacious than wild-type phage at attacking biofilm despite being made with a modified T7 phage, I also treated biofilm with wild-type T7 ($T7_{wt}$) or wild-type T3 ($T3_{wt}$) (Figure 3a). After 24 h of treatment, CV staining of untreated biofilm had a 600 nm absorbance (A_{600}) approximately equal to that for $T7_{wt}$-treated biofilm (Figure 3a). Both $T3_{wt}$-treated biofilm and $T7_{control}$-treated biofilm were much reduced compared with the untreated biofilm: the former had an A_{600} that was lower than that of untreated biofilm by a factor of 10.3, while the latter had an A_{600} that was lower than that of untreated biofilm by a factor of 5.6 (Figure 3a). The amount of biofilm left on the $T7_{DspB}$-treated pegs was the least of all the treatment types, with an A_{600} which was less by a factor of 14.5 than that of untreated biofilm and less by a factor of 2.6 than that of $T7_{control}$-treated biofilm ($P = 5.4*10^{-8}$). These findings demonstrate that DspB expression in $T7_{DspB}$ is crucial to elevating its biofilm-removing efficacy over that of wild-type phage and non-enzymatic $T7_{control}$ phage (Figure 3a).

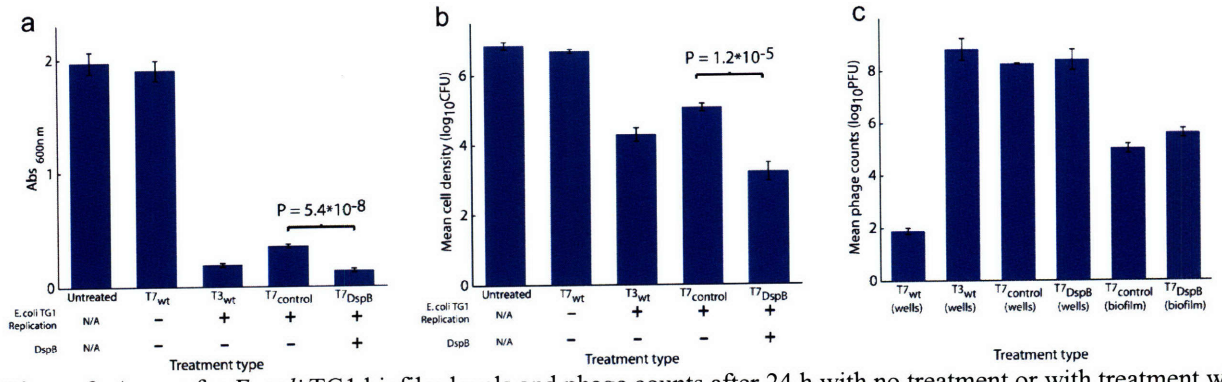

Figure 3. Assays for *E. coli* TG1 biofilm levels and phage counts after 24 h with no treatment or with treatment with wild-type phage $T7_{wt}$, wild-type phage $T3_{wt}$, non-DspB-expressing control phage $T7_{control}$, or DspB-expressing phage $T7_{DspB}$. Error bars indicate s.e.m. **(a)** Mean absorbance (600 nm) for $n = 16$ biofilm pegs stained with 1% CV, solubilized in 33% acetic acid, and diluted 1:3 in 1x PBS (62). **(b)** Mean cell densities (log_{10}(CFU/peg)) for $n = 12$ biofilm pegs. Pegs treated with $T7_{DspB}$ resulted in a 3.65 log_{10}(CFU/peg) reduction in viable cells recovered from *E. coli* biofilm compared to untreated biofilm. **(c)** Mean phage counts (log_{10}(PFU/peg)) recovered from media in $n = 3$ microtiter plate wells (wells) or sonication of $n = 3$ biofilm pegs (biofilm), as indicated, after 24 h of treatment with initial inoculations of 10^3 PFU/well. Both $T7_{control}$ and $T7_{DspB}$ showed evidence of replication with phage counts obtained from the microtiter plate wells or with phage counts recovered from the biofilms after sonication. Adapted from Ref. (42).

To confirm that the decrease in CV staining corresponded with killing of biofilm cells, I used sonication to obtain viable cell counts (CFU/peg) for bacteria surviving in the biofilms after phage treatment. Pre-grown TG1(*lacI*::*kan*) biofilm (prior to treatment) reached a mean cell density of 6.4 log_{10}(CFU/peg) after 24 h of growth (Figure 3b). After 24 h of additional growth in new LB media with no phage treatment, the untreated biofilm had a mean cell density of 6.9 log_{10}(CFU/peg) (Figure 3b). $T3_{wt}$-treated biofilm had a mean cell density that was less than that of $T7_{control}$-treated biofilm by a factor of 5.9 and greater than that of $T7_{DspB}$-treated biofilm by a factor of 12 (Figure 3b). $T7_{control}$-treated biofilm had a mean cell density of 5.1 log_{10}(CFU/peg) while the mean cell density for $T7_{DspB}$-treated biofilm was 3.2 log_{10}(CFU/peg), the lowest of all the treatment types (Figure 3b). The difference in viable cells recovered from $T7_{control}$-treated biofilm and $T7_{DspB}$-treated biofilm was statistically significant ($P = 1.2*10^{-5}$). These results are consistent with the CV staining data and demonstrate that DspB-expressing $T7_{DspB}$ phage are substantially more effective at killing *E. coli* TG1 biofilm compared with wild-type $T3_{wt}$, wild-type $T7_{wt}$, and non-DspB-expressing control $T7_{control}$ phage.

Our two-pronged method of biofilm eradication involves expression of DspB and rapid phage replication (Figure 1). To confirm that our phage multiplied, I obtained PFU counts from media in the microtiter plate wells. By 24 h of treatment, wild-type T7 had not replicated but wild-type T3 had multiplied significantly within the biofilm (Figure 3c). To compare the amount of phage in the microtiter plate wells with phage residing in the biofilms, I also obtained PFU counts by sonicating the biofilms. After 24 h of treatment, PFU counts for $T7_{control}$ and $T7_{DspB}$ recovered from the microtiter plate wells were several orders of magnitude greater than PFU counts recovered by sonication of the biofilms (Figure 3c). Overall, PFU counts obtained from the wells and the biofilms were all orders of magnitude greater than the initial inoculation of 10^3 PFU, confirming that phage multiplication indeed took place (Figure 3c).

2.2.3 Time Courses and Dose-Responses for Enzymatically-Active Bacteriophage Treatment

Since I determined that $T7_{DspB}$ had greater biofilm-removing capability than $T7_{control}$ after 24 h of infection, I next sought to determine the time course of biofilm destruction. As shown in Figure 4a, by 5 h post-infection, $T7_{DspB}$-treated biofilm had a mean cell density that was 0.82 $\log_{10}$(CFU/peg) less than $T7_{control}$-treated biofilm ($P = 2.0*10^{-4}$). At 10 h post-infection, $T7_{DspB}$-treated biofilm began to settle at a steady-state mean cell density between 3 to 4 $\log_{10}$(CFU/peg), while $T7_{control}$-treated biofilm flattened out at approximately 5 $\log_{10}$(CFU/peg) by 20 h post-infection (Figure 4a). $T7_{DspB}$-treated biofilms had mean cell densities that were approximately two orders of magnitude lower than $T7_{control}$-treated biofilms, up to 48 h of total treatment (Figure 4a), and importantly, $T7_{DspB}$ treatment reduced biofilm levels by about 99.997% (4.5 $\log_{10}$(CFU/peg)) compared with untreated biofilm. I found no evidence of phage resistance developing over the long time course of treatment (Figure 4a).

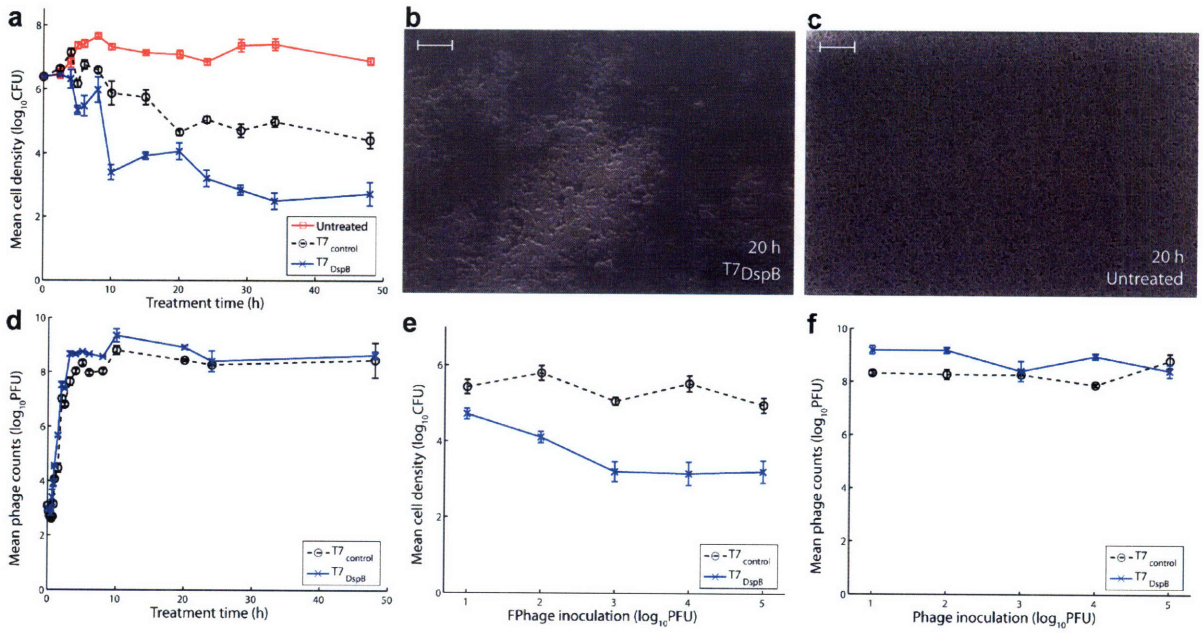

Figure 4. Time-course curves, dosage response curves, and SEM images for engineered phage treatment targeting E. coli TG1 biofilm. Scale bars are 10 μm. Each data point in parts **(a)** and **(e)** represents the mean $\log_{10}$-transformed cell density of n = 12 biofilm pegs. Each data point in parts **(d)** and **(f)** represents the mean $\log_{10}$-transformed phage counts obtained from n = 3 microtiter plate wells. Error bars indicate s.e.m. **(a)** Time course (up to 48 h) of viable cell counts for no treatment (red squares), treatment with $T7_{control}$ (black circles), or treatment with $T7_{DspB}$ (blue crosses) demonstrates that $T7_{DspB}$ significantly reduced biofilm levels compared with $T7_{control}$. **(b)** SEM image of $T7_{DspB}$-treated biofilm after 20 h shows significant disruption of the bacterial biofilm. **(c)** SEM image of untreated biofilm after 20 h shows a dense biofilm. **(d)** Time course of phage counts obtained after initial inoculation of E. coli TG1 biofilm with 10^3 PFU/well of $T7_{control}$ (black circles) or $T7_{DspB}$ (blue crosses). Both $T7_{control}$ and $T7_{DspB}$ began to replicate rapidly after initial inoculation. **(e)** Dose response curves of mean cell densities (measured after 24 h of treatment) for $T7_{control}$ (black circles) and $T7_{DspB}$ (blue crosses). For all initial phage inoculations, $T7_{DspB}$-treated biofilm had significantly lower mean cell densities compared to $T7_{control}$-treated biofilm. **(f)** Dose response curves of mean phage counts (measured after 24 h of treatment) for $T7_{control}$ (black circles) and $T7_{DspB}$ (blue crosses). For all initial phage inoculations, both $T7_{control}$ and $T7_{DspB}$ multiplied significantly. Adapted from Ref. (42).

I also used scanning electron microscopy (SEM) to image the biofilm pegs over the time course of phage treatment in order to directly visualize biofilm dispersal by our enzymatically-active phage (Figure 4b, Figure 4c, and Figure 5). After 20 h of treatment, $T7_{DspB}$-treated biofilm (Figure 4b) was significantly disrupted compared with the untreated biofilm (Figure 4c). These results confirm that $T7_{DspB}$ indeed causes biofilm reduction and bacterial cell killing.

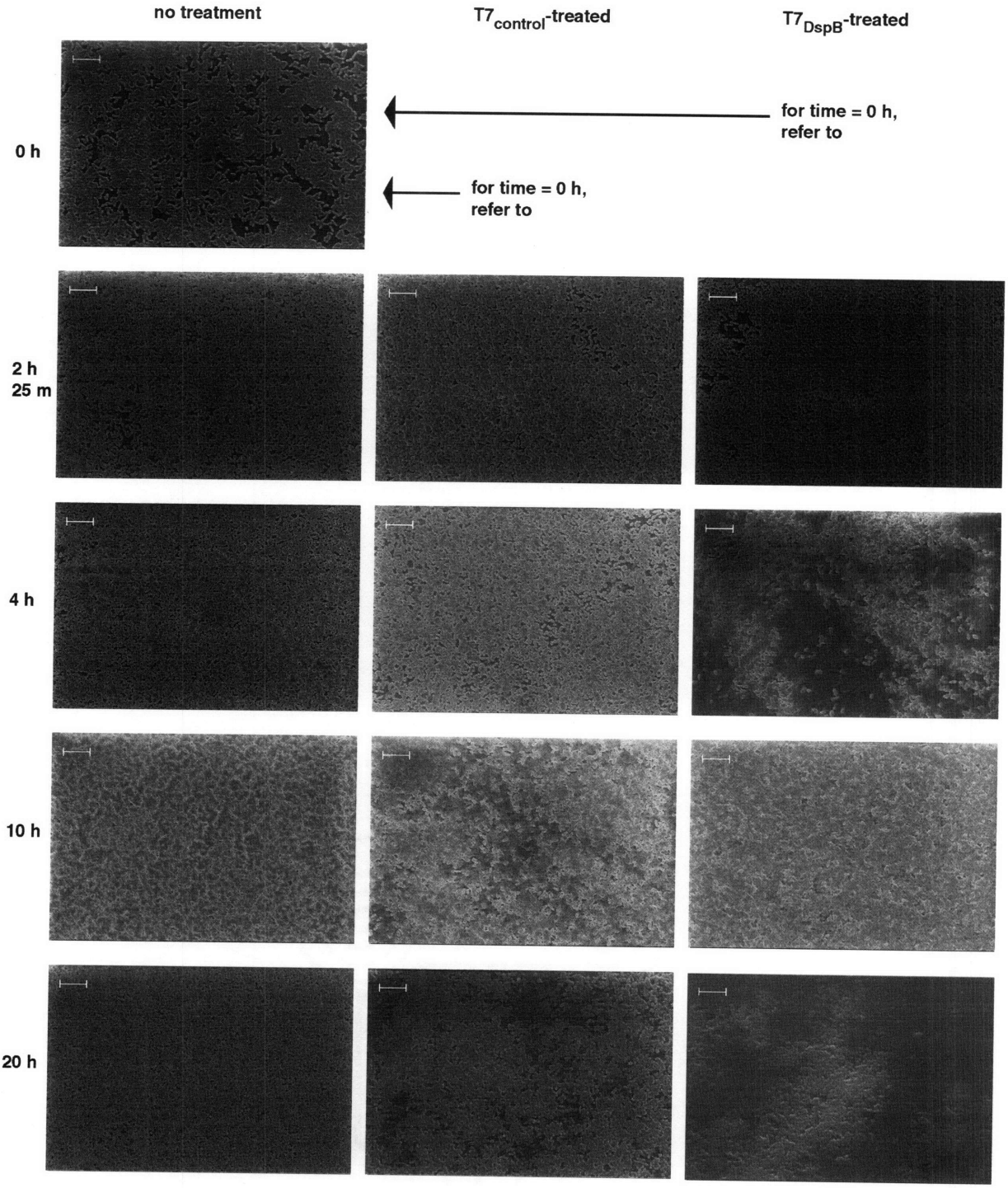

Figure 5. Scanning electron microscopy images for untreated, $T7_{control}$-treated, and $T7_{DspB}$-treated biofilms. Scale bars are 10 μm. Consistent with time-course data (**Figure 4a**), $T7_{DspB}$-treated biofilm and $T7_{control}$-treated biofilm were indistinguishable from untreated biofilm at 2 h 25 min post-infection. However, by 4 h post-infection, $T7_{DspB}$-treated biofilm began to lyse and disperse significantly, while $T7_{control}$-treated biofilm was still largely undisturbed. By 10 h post-infection, significant amounts of cell debris were seen in both $T7_{control}$-treated and $T7_{DspB}$-treated biofilms. At 20 h post-infection, $T7_{control}$-treated and $T7_{DspB}$-treated biofilms had been disrupted by phage treatment, but $T7_{DspB}$-treated biofilm was composed largely of cell debris and had fewer intact cells than $T7_{control}$-treated biofilm. Adapted from Ref. (42).

To verify that phage replication was occurring over time, I obtained PFU counts in the microtiter wells. As seen in Figure 4d, both $T7_{control}$ and $T7_{DspB}$ began to replicate within the bacterial biofilm as early as 50 minutes post-infection. By about 190 minutes, $T7_{control}$ and $T7_{DspB}$ PFU/peg approached steady-state levels of approximately 8 to 9 $\log_{10}$(PFU/peg), indicating that phage replication had occurred (Figure 4d). $T7_{DspB}$ PFU/peg were generally higher than $T7_{control}$ PFU/peg but not by orders of magnitude as was the case for CFU counts per peg. This is because the T7 burst size (~250 PFU per infective center) (63) multiplied by the number of the extra cells killed by $T7_{DspB}$, compared with $T7_{control}$, equals extra PFU/peg that are insignificant compared with the PFU levels already reached by $T7_{control}$. I did not note any significant differences in burst sizes and growth rates between $T7_{DspB}$ and $T7_{control}$ (data not shown).

Considering that the above experiments were carried out with initial inoculations of 10^3 PFU/peg, which translates to a multiplicity of infection (MOI) of about $1:10^{3.4}$ (Figure 4a), I next aimed to determine the effect of changing the initial MOI on biofilm removal. With low phage doses, repeated rounds of phage multiplication and DspB expression should promote biofilm dispersal and allow more bacterial cells to be accessible for subsequent phage infection. With high phage doses, initial DspB production post-infection should also be very disruptive to biofilm integrity. As shown in Figure 4e, $T7_{DspB}$ was more effective than $T7_{control}$ at removing biofilm at all inoculation levels tested, ranging from 10^1 PFU/peg to 10^5 PFU/peg. A dose-dependent effect of phage inoculation on biofilm destruction was observed, with larger inoculations leading to lower mean cell densities, particularly for $T7_{DspB}$ (Figure 4e). At inoculation levels greater than or equal to 10^2 PFU/peg, mean cell densities (CFU/peg) for $T7_{DspB}$-treated biofilm were significantly lower than those for $T7_{control}$-treated biofilm by a factor

of 49–232 (Figure 4e). Thus, at low and high initial inoculations, DspB-expressing T7 is more efficacious at disrupting *E. coli* TG1 biofilm compared with non-DspB-expressing control T7. Note also that all phage dosages tested exhibited phage multiplication within the biofilm (Figure 4f). These results together suggest that DspB-expressing phage may have improved efficacy in real-world situations where the ability to deliver high levels of phage to biofilms may be limited or where sustained phage replication is less likely, e.g., in the gastrointestinal tract of cholera patients (29, 30).

2.3 Discussion

In this work, I demonstrated that engineered phage which express biofilm-degrading enzymes are more efficacious at removing bacterial biofilms than non-enzymatic phage alone. Though our results were obtained for a prototype, proof-of-principle phage, I believe that our design can be adapted to work in other phage and with other biofilm-degrading enzymes to target a wide range of biofilms. Thus, engineered bacteriophage treatment should be considered as an addition to the therapies available for use against bacterial biofilms in medical, industrial, and biotechnological settings (28). Future improvements to this design may include directed evolution for optimal enzyme activity, delaying cell lysis or using multiple phage promoters to allow for increased enzyme production, targeting multiple biofilm EPS components with different proteins as well as targeting multi-species biofilm with a cocktail of different species-specific engineered enzymatically-active phage, and combination therapy with antibiotics and phage to improve the efficacy of both types of treatment.

Phage therapy has begun to be accepted in industrial and biotechnological settings. For example, the FDA recently approved the use of phage targeted at *Listeria monocytogenes* as a food additive (27). However, phage therapy has several challenges that must be overcome

before it will be accepted in Western medicine for treating humans (28). These problems include the lack of properly designed clinical trials to date (28), development of phage resistance (11, 12, 29), phage immunogenicity in the human body and clearance by the reticuloendothelial system (RES) (11, 30), the release of toxins upon bacterial lysis (11), and phage specificity (11). Fortunately, many of these concerns are currently being studied and addressed. For example, combination therapy with antibiotics and phage may alleviate the development of phage resistance (11, 12, 29). Long-circulating phage can be isolated that can avoid RES clearance to increase *in vivo* efficacy (30). The problem of phage clearance is an important one that needs to be solved as it may make phage therapy more useful for treating transient infections rather than chronic ones. Non-lytic and non-replicative phage have been engineered to kill bacteria while minimizing endotoxin release (31, 32). Progress is also being made in the development of toxin-free phage preparations (33).

The specificity of phage for host bacteria is both an advantage and a disadvantage for phage therapy. Specificity allows human cells as well as innocuous bacteria to be spared, potentially avoiding serious issues such as drug toxicity or *Clostridium difficile* overgrowth that can arise with antibiotic use. *C. difficile* infection is characterized by diarrhea and colitis, and has increased in severity in recent years (34). Antibiotic therapy is believed to alter the microbial flora in the colon due to lack of target specificity, thus allowing *C. difficile* to proliferate and cause disease (35). Furthermore, the ability of our engineered phage to utilize the local bacterial synthetic machinery to produce biofilm-degrading enzymes means that exogenously-applied enzymes, which could have unintended effects on off-target biofilms, are not needed. However, host specificity means that a well-characterized library of phage must be maintained so that an appropriate therapy can be designed for each individual infection (11).

The diversity of bacterial infections implies that it may be difficult for any particular engineered phage to be a therapeutic solution for a wide range of biofilms. Indeed, phage therapy generally requires the use of phage cocktails to cover a range of target bacteria.

Overcoming the difficulty of creating a collection of enzymatically-active engineered phage is a problem that can be solved by new cost-effective, large-scale DNA sequencing and DNA synthesis technologies (37, 64, 65). Sequencing technologies will allow the characterization of collections of natural phage that have been used in phage typing and phage therapy for many years (66, 67). Once these phage have been better understood, synthesis technologies should enable the addition of biofilm-degrading enzymes to produce new, modified phage. Furthermore, rational engineering methods with new synthesis technologies can be employed to broaden phage host range. For example, T7 has been modified to express K1-5 endosialidase, allowing it to effectively replicate in *E. coli* that produce the K1 polysaccharide capsule (48). In this study, I took advantage of gene *1.2* from phage T3 to extend our phage host range to include *E. coli* that contain the F plasmid, thus demonstrating that multiple modifications of a phage genome can be done without significant impairment of the phage's ability to replicate (61). *Bordetella* bacteriophage use an intriguing reverse-transcriptase-mediated mechanism to produce diversity in host tropism which may provide inspiration for future designs (68, 69). In addition, utilizing enzymes, such as DspB, that target important adhesins which are common to a broad range of bacterial species, including clinical strains, should also help enzymatically-active phage be applicable to a greater number of infections (49, 51). Along these lines, the many biofilm-promoting factors required by *E. coli* K-12 to produce a mature biofilm are likely to be shared among different biofilm-forming bacterial strains and are thus potential targets for engineered enzymatic bacteriophage (60).

2.4 Conclusions

Because antibiotic resistance in biofilms poses a significant hurdle to eliminating biofilms with conventional antimicrobial drugs, new anti-biofilm strategies, such as phage therapy, should be explored. Novel synthetic biology technologies should enable the engineering of natural phage with biofilm-degrading enzymes to produce libraries of enzymatically-active phage, which could complement efforts to screen for new biofilm-degrading bacteriophages in the environment. Once bacteriophage therapy itself becomes better understood and utilized, engineered bacteriophage with biofilm-degrading enzymatic activity could become a viable option in meeting the challenge of biofilm control in environmental, industrial, and clinical settings.

2.5 Materials and Methods

2.5.1 Bacterial strains, bacteriophage, and chemicals.

E. coli TG1 (F'*traD36 lacI*^{q}Δ(*lacZ*) *M15 proA*$^+$*B*$^+$/*supE* Δ(*hsdM-mcrB*)*5* (r_k^- m_k^- McrB$^-$) *thi* Δ(*lac-proAB*)) was obtained from Zymo Research (Orange, CA). The strain TG1 *(lacI::kan)* used to grow biofilm was created by one-step inactivation of the *lacI* gene by a kanamycin-resistance cassette (70). *E. coli* BL21 was obtained from Novagen Inc. (San Diego, CA). Wild-type T7 (ATCC #BAA-1025-B2) and T3 (ATCC #11303-B3) were purchased from ATCC (Manassas, VA). T4 DNA ligase and all restriction enzymes were obtained from New England Biolabs, Inc. (Ipswich, MA). PCR reactions were carried out using PCR SuperMix High Fidelity from Invitrogen (Carlsbad, CA). Restriction digests of T7 genomic DNA were purified with the QIAEX II kit, while purification of all other PCR reactions and restriction digests was carried out with the QIAquick Gel Extraction or PCR Purification kits (Qiagen, Valencia, CA). All other chemicals were purchased from Fisher Scientific, Inc. (Hampton, NH).

2.5.2 Construction and purification of engineered phage

Our engineered T7 phage was created using the T7select415-1 phage display system (Novagen). Instead of cloning DspB onto the phage surface, I designed the T7select phage to express DspB intracellularly during infection. The *dspB* gene was cloned from *Actinobacillus actinomycetemcomitans* genomic DNA (ATCC #700685D) into the pET-9a plasmid (Novagen) under the control of the strong T7 φ10 promoter in between the NdeI and BamHI sites using the forward primer 5' atataatc catatg aat tgt tgc gta aaa ggc aat tc 3' and reverse primer 5' atatac ggatcc tca ctc atc ccc att cgt ct 3' (restriction sites underlined). I placed a stop codon in all three reading frames downstream of the T7select415-1 *10B* capsid gene followed by the φ10-*dspB* construct, so *dspB* would be strongly transcribed by T7 RNA polymerase during infection (Figure 2b). The φ10-*dspB* construct was isolated by PCR with the primers 5' gTA AcT AA cgaaattaat acgactcact atagg 3' and 5' atataa cggccg c aagctt tca ctc atc ccc att cgt ct 3' (stop codons in uppercase letters); the product was used in a subsequent PCR reaction with the primers 5' tactc gaattc t TAA gTA AcT AA cgaaattaat acgactc 3' and 5' atataa cggccg c aagctt tca ctc atc ccc att cgt ct 3' to create a construct beginning with stop codons in each reading frame followed by the φ10-*dspB* construct. Both the product of this PCR reaction and the T7select415-1 DNA were digested with EcoRI and EagI, purified, ligated together using T4 DNA ligase, and packaged into T7 phage particles with T7select packaging extracts to create phage $T7_{DspB\text{-}precursor}$. The control phage, $T7_{control\text{-}precursor}$, was constructed by cloning the T7select control *S·Tag* insert into the T7select415-1 phage genome and packaging the genome using T7select packaging extracts (Figure 2c). Phage $T7_{DspB\text{-}precursor}$ and $T7_{control\text{-}precursor}$ were routinely amplified on *E. coli* BL21 and verified by DNA sequencing.

Since wild-type T7 is unable to replicate normally in F-plasmid-containing *E. coli*, I cloned gene *1.2* from phage T3 into $T7_{DspB\text{-}precursor}$ and $T7_{control\text{-}precursor}$ to create $T7_{DspB}$ and $T7_{control}$, respectively, which are able to escape exclusion by the F plasmid (Figure 2b and Figure 2c) (61). Genomic DNA from $T7_{DspB\text{-}precursor}$ and $T7_{control\text{-}precursor}$ was isolated using the Qiagen Lambda Midi Kit. T3 gene *1.2* was cloned from the T3 genome using primers 5' cgta tgatca aacg agcagggcga acagtg 3' and 5' cgta tgatca ccactc gttaaagtga ccttaaggat tc 3' and inserted into the unique BclI site in both the $T7_{DspB\text{-}precursor}$ and $T7_{control\text{-}precursor}$, which were then packaged with T7select packaging extracts. The resulting phage were amplified on *E. coli* BL21 and then plated on *E. coli* TG1(*lacI*::*kan*) to isolate $T7_{DspB}$ (Figure 2b) and $T7_{control}$ (Figure 2c), which were confirmed by PCR to have gene *1.2* from T3.

Prior to biofilm treatment, $T7_{DspB}$ and $T7_{control}$ were amplified on *E. coli* BL21 and purified. 12 mL of BL21 overnight cultures were diluted with 12 mL of LB in 125 mL flasks, inoculated with 30 μL of high-titer phage stock, and allowed to lyse at 37°C and 300 rpm for 3 h. Lysed cultures were clarified by centrifuging for 10 minutes at 10,000*g* and filtering the supernatants through Nalgene #190-2520 0.2 μm filters (Nalge Nunc International, Rochester, NY). The purified solutions were centrifuged in a Beckman SW.41T rotor for 1 h at 29,600 rpm to concentrate the phage. The supernatants were removed and pellets were resuspended in 0.2 M NaCl, 2 mM Tris-HCl pH 8.0, and 0.2 mM EDTA. Phage suspensions were reclarified in tabletop microcentrifuges at maximum speed (~13,200 rpm) for 10 minutes. The purified supernatants were finally diluted in 0.2 M NaCl, 2 mM Tris-HCl pH 8.0, and 0.2 mM EDTA for treatment. Appropriate amounts of phage were added to LB + kanamycin (30 μg/mL) for treatment, as described below. Phage purified by this protocol were no more effective at

reducing bacterial biofilm levels compared with phage purified by centrifugation with CsCl step gradients (data not shown).

All phage PFU counts were determined by combining phage with 300 μL of overnight *E. coli* BL21 culture and 4-5 mL of 50°C LB top agar (0.7% w/v agar). This solution was mixed thoroughly, poured onto LB agar plates, inverted after hardening, and incubated for 4-6 h at 37°C until plaques were clearly visible.

2.5.3 Biofilm growth and treatment

All experiments were performed in LB media + kanamycin (30 μg/mL). *E. coli* biofilms were grown with the MBEC Physiology & Genetics Assay (MBEC BioProducts Inc., Edmonton, Canada), which consists of a 96-peg lid that fits into a standard 96-well microtiter plate. Each well was inoculated with 150 μL of media containing 1:200 dilutions of overnight cultures which had been grown at 37°C and 300 rpm. Control wells with only media but no bacteria were included. MBEC lids were placed in the microtiter plates, inserted into plastic bags to prevent evaporation, and placed in a shaker (HT Infors Minitron) for 24 h at 35°C and 150 rpm to form biofilm on the pegs.

For all treatments except for the dose response experiment, 10^3 PFU of phage were combined with 200 μL LB + kanamycin (30 μg/mL) in each well in new microtiter plates (COSTAR #3370). For the dose response experiment, 10^1, 10^2, 10^3, 10^4, or 10^5 PFU were combined with 200 μL LB + kanamycin (30 μg/mL) in each well. Wells with only media but no phage were included as untreated biofilm controls. MBEC lids with 24 h pre-grown *E. coli* biofilm were removed from their old 96-well microtiter plates, and placed into the new microtiter plates and back into plastic bags in a shaker at 35°C and 150 rpm for treatment. After specified

amounts of time for the time-course experiment or 24 h for all other experiments, MBEC lids were removed and the amounts of biofilm remaining were assayed by CV staining or viable cell counting, as described below.

2.5.4 Crystal violet staining assay

Crystal violet staining of MBEC pegs was carried out, after rinsing three times with 1x phosphate-buffered saline (PBS), using a standard, previously reported protocol (62). MBEC pegs were rinsed three times with 200 μL of 1x phosphate-buffered saline (PBS) and placed into fresh microtiter plates with wells containing 200 μL of 1% CV. After 15 minutes of incubation at room temperature, the stained MBEC pegs were washed three times with 200 μL of 1x PBS and placed into fresh microtiter plates containing 200 μL of 33% acetic acid to solubilize the dye for 15 minutes (62). To avoid oversaturating the absorbance detector, 66.7 μL of the solubilized dye was added to 133.3 μL of 1x PBS; the absorbance at 600 nm of this mixture was assayed in a TECAN SpectraFluor Plus plate reader (Zurich, Switzerland). The mean A_{600nm} of wells corresponding to pegs with no biofilm growth was used as a blank measurement to correct all other A_{600nm} absorbances.

2.5.5 Viable cell count assay

I obtained viable cell counts by disrupting biofilms on the pegs in a sonicating water bath. MBEC pegs were first rinsed three times with 200 μL of 1x PBS and placed into fresh microtiter plates (NUNC #262162) containing 145 μL of 1x PBS in each well, which completely covered the biofilms growing on the pegs. To prevent further infection of bacteria by phage, 20 ng of T7 Tail Fiber Monoclonal Antibody (Novagen) was added to each well. MBEC lids and plates were placed in a Branson Ultrasonics #5510 sonic water bath (Danbury, CT) and sonicated for 30 minutes at 40 kHz to dislodge bacteria in biofilms into the wells. Serial dilutions were

performed and plated on LB agar + kanamycin (30 μg/mL) plates. Colony-forming units were counted after overnight incubation at 37°C.

2.5.6 Scanning electron microscopy

SEM was performed according to MBEC recommendations (71). Scanning electron microscopy was carried out with a Carl Zeiss Supra 40 VP SEM using Carl Zeiss SmartSEM V05.01.08 software. Biofilm pegs were broken off at indicated time points and washed three times in 1x PBS. The pegs were then fixed in 2.5% glutaraldehyde in 0.1 M cacodylic acid (pH 7.2) for 2 to 3 h at room temperature. Subsequently, the pegs were air dried for at least 120 h, and mounted and examined by SEM in VPSE mode with EHT = 7.5 kV. Each peg was examined at several locations prior to imaging to ensure that characteristic images were acquired. Images were frame- or line-integrated using the SmartSEM software to achieve better resolution.

2.5.7 Phage counts

At indicated time points (Figure 4d) or after 24 h of treatment (Figure 3c and Figure 4f), media from $n = 3$ microtiter wells for each treatment type were serially diluted to obtain PFU counts for phage in the liquid phase. To obtain PFU counts for phage residing in biofilms at 24 h post-infection (Figure 3c), MBEC pegs were rinsed three times with 200 μL of 1x phosphate-buffered saline (PBS) and placed into fresh microtiter plates (NUNC #262162) containing 145 μL of 1x PBS in each well, which completely covered the biofilm on the pegs. No T7 Tail Fiber Monoclonal Antibody was added. The MBEC lids and plates were placed in a Branson Ultrasonics #5510 sonic water bath (Danbury, CT) and sonicated for 30 minutes at 40 kHz to dislodge bacteria and phage residing in biofilms into wells. Serial dilutions were performed to obtain PFU counts for phage in biofilms.

2.5.8 Statistical analysis

Student's unpaired two-sided t-test was used to test for statistical significance. For the CV staining assays, the dataset size for each treatment type was $n = 16$; for the CFU assays, $n = 12$ pegs per treatment type were used. Data for time-course CFU counts were collected from three independent experiments; all other CFU data were obtained from single experiments in time. Absorbances from crystal violet staining assays or CFU counts from viable cell count assays were evaluated for statistically significant differences using Student's unpaired two-sided t-test (assuming unknown and unequal variances) with an alpha level of 0.05 implemented in Matlab version 7.0.01 (Mathworks, Natick, MA). All CFU data were $\log_{10}$-transformed prior to analysis. All absorbance data and $\log_{10}$-transformed CFU data were verified to be approximately normally distributed using the qqplot() function in Matlab version 7.0.1 to meet the assumptions of the t-test. Error bars in figures indicate standard error of the mean (s.e.m).

3 NATURAL AND ENGINEERED BACTERIOPHAGE AS ADJUVANTS FOR ANTIBIOTIC THERAPY

3.1 Introduction

Bacteria rapidly develop resistance to antibiotics within years of first clinical use (72). Since antimicrobial drug development is increasingly lagging behind the evolution of antibiotic resistance, there is a pressing need for new antibacterial therapies which can be readily designed and implemented (1). In this work, I engineered a bacteriophage-based synthetic biology platform to overexpress target proteins and attack gene networks which are not directly targeted by antibiotics. This strategy allows the rapid translation of identified targets into effective antibiotic adjuvants to treat bacterial infections. Combination treatment with engineered bacteriophage and antibiotics greatly improves antibiotic efficacy in Escherichia coli. I show that suppressing the SOS network with engineered bacteriophage enhances killing by quinolones by over 2.7 and 4.5 orders of magnitude compared with control bacteriophage plus ofloxacin and ofloxacin alone, respectively. In addition, engineered bacteriophage can improve the killing of persister cells and biofilm cells, reduce the number of antibiotic-resistant bacteria in a antibiotic-treated population, and act as a strong adjuvant for other bactericidal antibiotics such as aminoglycosides and β-lactams. Finally, I show that bacteriophage which target one or more non-SOS gene networks are also useful antibiotic adjuvants.

Antibiotic resistance can be acquired genetically or result from persistence, in which a small fraction of cells in a population exhibits a non-inherited, phenotypic tolerance to antimicrobials (8, 21-24, 73-75). Acquired antibiotic resistance arises from mutations in antibiotic targets or from genes encoding proteins that pump antibiotics out of cells or inactivate antibiotics (7). Horizontal gene transfer can occur via transformation, conjugative plasmids, or

conjugative transposons and is responsible for spreading genes conferring resistance to antibiotics such as vancomycin and methicillin (19, 20, 76). Antibiotics that induce the SOS response, such as ciprofloxacin, can promote the mobilization of antibiotic-resistance genes (77, 78). Resistance genes that develop in non-clinical settings, such as in agriculture for livestock, may be subsequently transmitted to bacterial populations which infect humans (19, 79). Bacteria can also survive antibiotic treatment by entering a metabolically-dormant state of persistence (8, 73, 74). Persisters constitute a reservoir of latent cells that can regrow once antibiotic treatment ceases and may be responsible for the increased antibiotic tolerance observed in bacterial biofilms, which are difficult-to-eradicate surface-associated communities (74). By surviving treatment, persisters may play an important role in mutating or acquiring antibiotic-resistance genes. The constant evolution of antibiotic resistance poses a serious challenge to the usefulness of today's antibiotic drugs (1, 9-12).

Several strategies have been proposed for managing antibiotic resistance and controlling infections. Surveillance and containment measures are useful but do not address the fundamental evolution of resistance (19). Cycling antibiotics may help control resistant organisms but is costly and may not be efficacious enough by itself (25, 80). Reducing the overprescribing of antibiotics has only moderately reduced antibiotic resistance (81). Efforts have been also made to lessen the use of antibiotics in farming but some use is inevitable (82). New classes of antibiotics and effective antimicrobial agents should be developed but few are in pharmaceutical pipelines (1, 16, 83). Phage therapy to kill bacteria has been in use since the early 20th century (16, 17). Bacteriophage can be chosen to lyse bacteria or can be modified to express lethal genes to cause cell death (31, 32, 84-86). However, phage which are directly lethal to their bacterial hosts can produce phage-resistant bacteria in short amounts of time (11, 12, 29, 31, 32).

Combination therapy with different antibiotics or antibiotics plus phage may enhance bacterial killing and reduce the incidence of antibiotic resistance (42, 87-89).

High-throughput methodologies combined with traditional molecular biology techniques have enabled the discovery of potential drug targets for new antibiotics or antibiotic adjuvants (42, 90-92). Translating these targets from identification to actual drug compounds requires a significant amount of additional work and investment. In addition, antibiotic drugs typically work by inhibiting protein activity and therefore cannot take advantage of targets which need to exhibit increased activity in order to achieve antimicrobial activity. As a result, there remains a significant gap between target identification and drug development. In this work, I engineered bacteriophage to overexpress proteins to target gene networks and enhance bacterial killing in combination therapy with antibiotics. By using increasingly cost-effective DNA synthesis technologies, engineered bacteriophage can be rapidly designed to translate target discoveries into antimicrobial adjuvants. I specifically targeted nonessential gene networks in *E. coli* which are not directly attacked by antibiotics to avoid imposing additional evolutionary pressures for antibiotic resistance. Instead, I chose proteins that are responsible for repairing cellular damage caused by antibiotics, controlling regulatory networks, or modulating sensitivity to antibiotics.

3.2 Results

3.2.1 Suppressing the SOS response with LexA3-producing Bacteriophage

Bactericidal antibiotics cause hydroxyl radical formation which leads to DNA, protein, and lipid damage and ultimately, cell death (91). DNA damage induces the SOS response which results in DNA repair (Figure 8a) (93, 94). Since *recA* knockouts disable the SOS response and increase bacterial killing by bactericidal antibiotics such as quinolones like ofloxacin, I first engineered M13mp18 bacteriophage to overexpress *lexA3*, a repressor of the SOS response, in

order to potentiate antibiotics in *E. coli* (95). I used M13mp18, a modified version of M13 phage, as our substrate since it is a non-lytic filamentous bacteriophage and can accommodate DNA insertions into its genome (Figure 6a) (96). Unmodified filamentous bacteriophage have been shown to augment antibiotic efficacy to some extent (97). To repress the SOS response, I placed the *lexA3* gene under the control of the synthetic $P_L$tetO promoter followed by a synthetic ribosome-binding sequence (RBS) and named this phage φ_{lexA3} (Figure 6b and Figure 8a) (91, 95, 98-100). I confirmed that φ_{lexA3} suppressed the SOS response induced by ofloxacin treatment by monitoring GFP fluorescence in wild-type *E. coli* EMG2 cells carrying a plasmid with an SOS-responsive promoter driving *gfp* expression (Figure 7) (91).

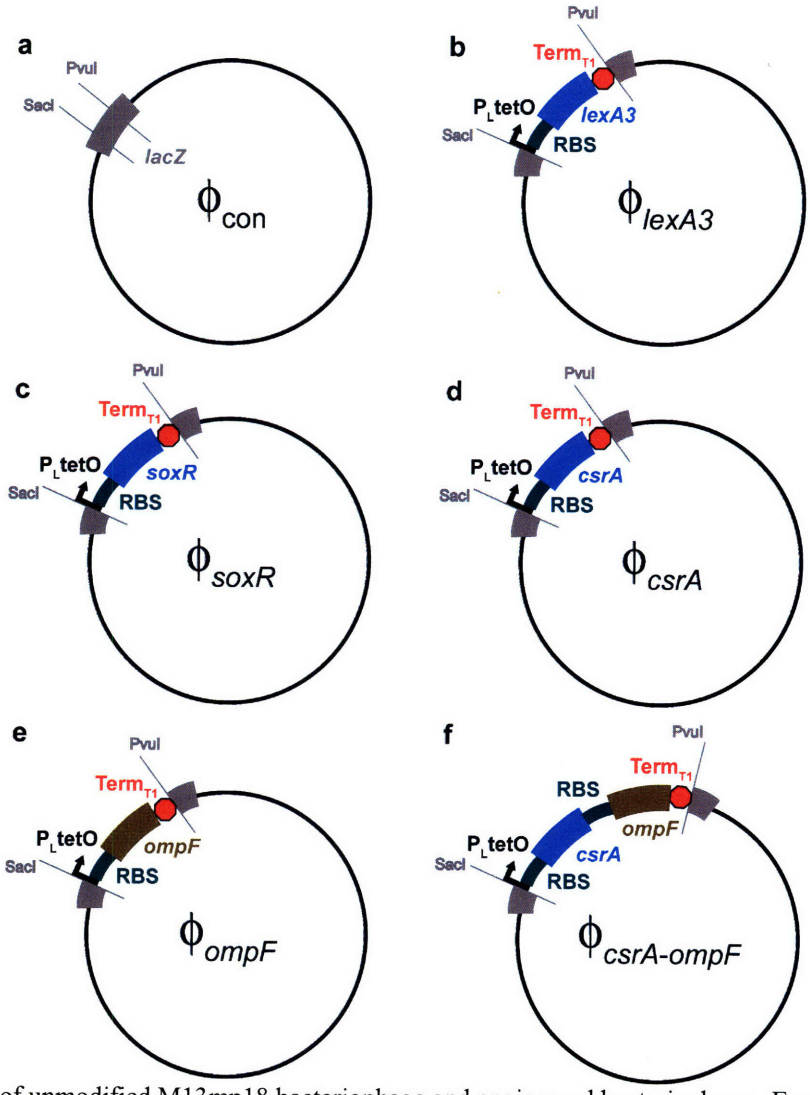

Figure 6. Genomes of unmodified M13mp18 bacteriophage and engineered bacteriophage. Engineered bacteriophage were constructed by inserting genetic modules under the control of a synthetic promoter and ribosome-binding sequence in between SacI and PvuI restriction sites. **(a)** Unmodified control M13mp18 (φ_{con}) contains *lacZ* to allow blue-white screening of engineered bacteriophage. **(b)** Engineered M13mp18 bacteriophage expressing *lexA3* (φ_{lexA3}). **(c)** Engineered M13mp18 bacteriophage expressing *soxR* (φ_{soxR}). **(d)** Engineered M13mp18 bacteriophage expressing *csrA* (φ_{csrA}). **(e)** Engineered M13mp18 bacteriophage expressing *ompF* (φ_{ompF}). **(f)** Engineered M13mp18 bacteriophage expressing *csrA* and *ompF* ($\varphi_{csrA\text{-}ompF}$).

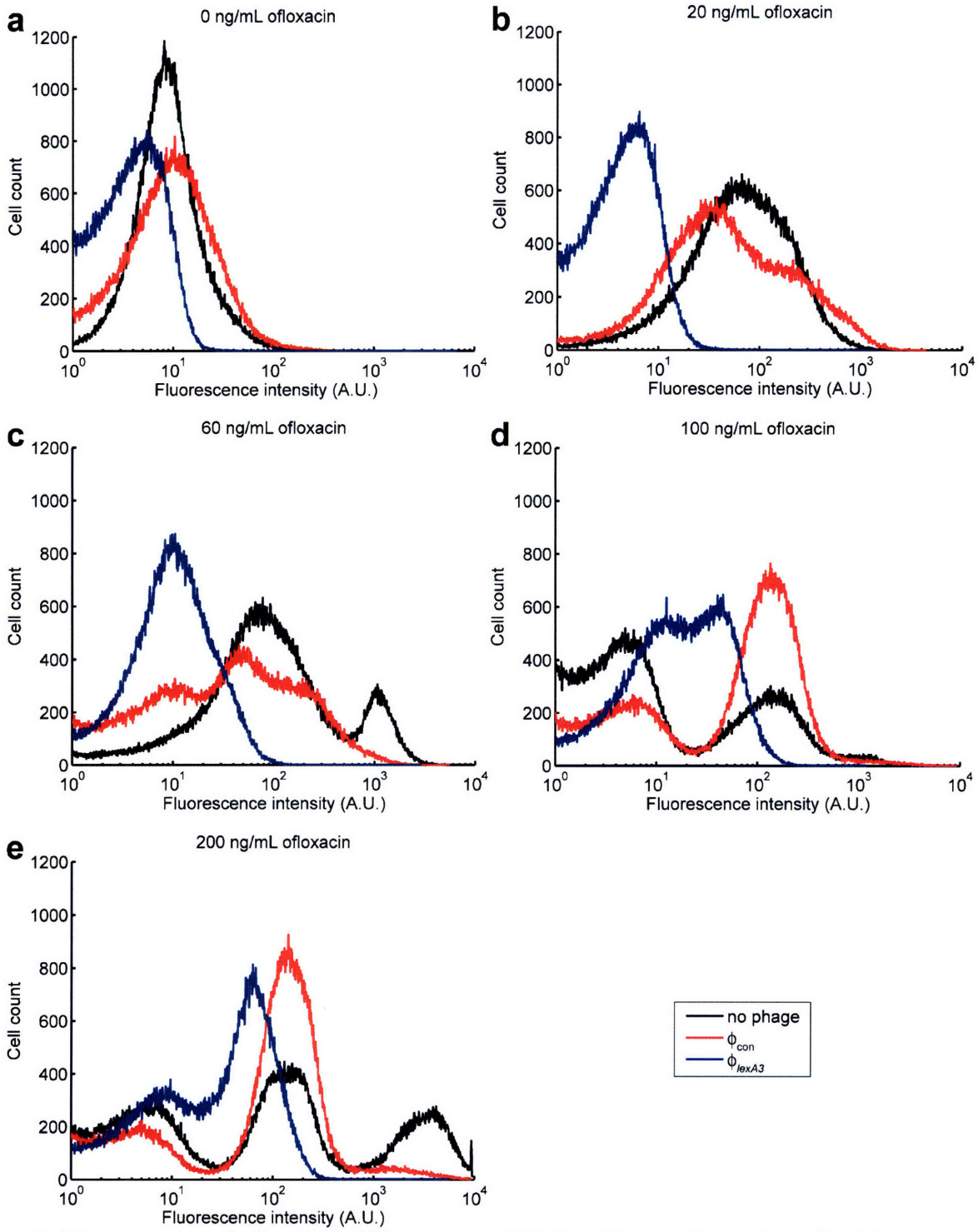

Figure 7. Flow cytometry of cells with an SOS-responsive GFP plasmid exposed to no phage (black lines), φ_{con} phage (red lines), or φ_{lexA3} phage (blue lines) for 6 hours with varying doses of ofloxacin. 10^8 plaque forming units per mL (PFU/mL) of phage were applied. Cells exposed to no phage or φ_{con} showed similar SOS induction profiles whereas cells with φ_{lexA3} exhibited significantly suppressed SOS responses. **(a)** 0 ng/mL ofloxacin treatment. **(b)** 20 ng/mL ofloxacin treatment. **(c)** 60 ng/mL ofloxacin treatment. **(d)** 100 ng/mL ofloxacin treatment. **(e)** 200 ng/mL ofloxacin treatment.

To test φ_{lexA3}'s adjuvant effect, I obtained time courses for bacterial killing with phage and/or ofloxacin treatment. I calculated viable cell counts by counting colony forming units (CFUs) during treatment with or without 10^8 plaque forming units/mL (PFU/mL) of bacteriophage and with or without 60 ng/mL ofloxacin (Figure 8b). Bacteria exposed only to ofloxacin were reduced by about 1.7 $\log_{10}$(CFU/mL) after 6 hours of treatment, reflecting the presence of persisters not killed by the drug (Figure 8b). By 6 hours, φ_{lexA3} improved the bactericidal effect of ofloxacin by 2.7 orders of magnitude compared to control φ_{con} (~99.8% additional killing) and over 4.5 orders of magnitude compared to no phage (~99.998% additional killing) (Figure 8b). Though bacterial growth resumed after 2 hours of treatment with unmodified φ_{con} or engineered φ_{lexA3} alone, no significant phage resistance developed when phage was used in combination with antibiotics (Figure 8b) (11, 12, 29, 31, 32). Thus, phage resistance should not limit the long-term usefulness of this design strategy. I confirmed that both φ_{con} and φ_{lexA3} bacteriophage replicated significantly during treatment (data not shown).

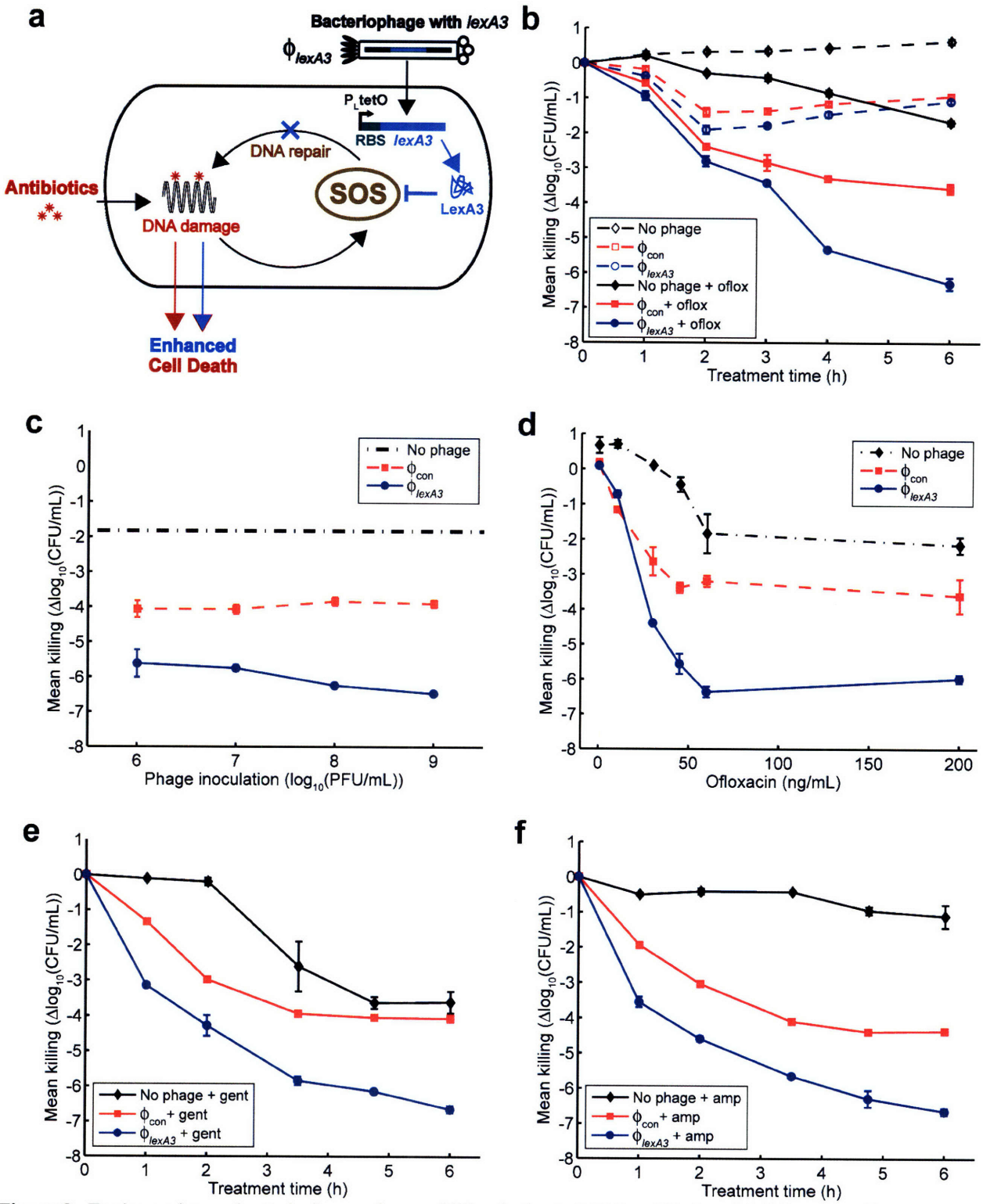

Figure 8. Engineered φ_{lexA3} bacteriophage enhances killing by bactericidal antibiotics. **(a)** Schematic of combination therapy with engineered bacteriophage and antibiotics. Bactericidal antibiotics induce DNA damage via hydroxyl radicals, leading to either cell death or induction of the SOS response followed by DNA repair and survival (91). Engineered phage carrying the *lexA3* gene (φ_{lexA3}) under the control of the synthetic promoter $P_L$tetO and a ribosome-binding sequence (99) acts as an antibiotic adjuvant by suppressing the SOS response due to DNA damage and increasing cell death. **(b)** Killing curves for no phage (black diamonds), unmodified φ_{con} phage (red

squares), and φ_{lexA3} (blue circles) without ofloxacin (dotted lines, open symbols) or with 60 ng/mL ofloxacin [oflox] (solid lines, closed symbols). 10^8 PFU/mL phage was used. φ_{lexA3} greatly enhanced killing by ofloxacin by 4 hours of treatment. **(c)** Phage dose response shows that φ_{lexA3} (blue circles with solid line) is a strong adjuvant for ofloxacin (60 ng/mL) over a wide range of initial inoculations compared with no phage (black dash-dotted line) and unmodified φ_{con} (red squares with dashed line). **(d)** Ofloxacin dose response shows that φ_{lexA3} (blue circles with solid line) improves killing even at low levels of drug compared with no phage (black diamonds with dash-dotted line) and unmodified φ_{con} (red squares with dashed line). 10^8 PFU/mL phage was used. **(e)** Killing curves for no phage (black diamonds), unmodified φ_{con} (red squares), and φ_{lexA3} (blue circles) with 5 μg/mL gentamicin [gent]. 10^9 PFU/mL phage was used. φ_{lexA3} phage greatly improved killing by gentamicin. **(f)** Killing curves for no phage (black diamonds), unmodified φ_{con} (red squares), and φ_{lexA3} (blue circles) with 5 μg/mL ampicillin [amp]. 10^9 PFU/mL phage was used. φ_{lexA3} phage greatly improved killing by ampicillin.

To verify that φ_{lexA3} is a useful antibiotic adjuvant in different situations, I assayed for bacterial killing with varying initial phage inoculation doses (Figure 8c) or varying doses of ofloxacin (Figure 8d) after 6 hours of treatment. Given that the starting concentration of bacteria was about 10^9 CFU/mL (data not shown), φ_{lexA3} enhanced ofloxacin's bactericidal activity over a wide range of multiplicity-of-infections (MOIs), from 1:1000 to 1:1 (Figure 8c). φ_{lexA3}'s ability to increase killing by ofloxacin at a low MOI reflects rapid replication and infection by M13 bacteriophage even with the burden of *lexA3* expression. For ofloxacin concentrations at 30 ng/mL and higher, φ_{lexA3} resulted in much greater killing compared with no phage or unmodified φ_{con} (Figure 8d). Thus, φ_{lexA3} is a strong adjuvant for ofloxacin at doses below and above the minimum inhibitory concentration (60 ng/mL, data not shown).

Next, I determined whether our engineered phage could increase killing by classes of antibiotics other than the quinolones. I tested φ_{lexA3}'s adjuvant effect for gentamicin, an aminoglycoside, and ampicillin, a β-lactam antibiotic. φ_{lexA3} increased gentamicin's bactericidal action by over 2.5 and 3 orders of magnitude compared with φ_{con} and no phage, respectively (Figure 8e). φ_{lexA3} also improved ampicillin's bactericidal effect by over 2.2 and 5.5 orders of magnitude compared with φ_{con} and no phage, respectively (Figure 8f). For both gentamicin and ampicillin, φ_{lexA3}'s strong adjuvant effect was noticeable after 1 hour of treatment (Figure 8e and Figure 8f). These results are consistent with previous observations that Δ*recA* mutants exhibit

increased susceptibility to quinolone, aminoglycoside, and β-lactam drugs (91). Therefore, engineered bacteriophage such as φ_{lexA3} can act as general adjuvants for three major classes of bactericidal drugs.

Engineered φ_{lexA3} bacteriophage is also capable of reducing the number of persister cells in populations already exposed to antibiotics as well as enhancing antibiotic efficacy against biofilms. For example, φ_{lexA3} added to a population previously treated only with ofloxacin increased the killing of bacteria which survived the initial treatment by over 0.94 and 1.3 orders of magnitude compared with unmodified φ_{con} and no phage, respectively (Figure 9). I also determined that engineered φ_{lexA3} was effective against bacteria living in biofilms. Simultaneous application of φ_{lexA3} and ofloxacin improved killing of biofilm cells by about 1.4 and 2.1 orders of magnitude compared with φ_{con} or no phage, respectively (Figure 10).

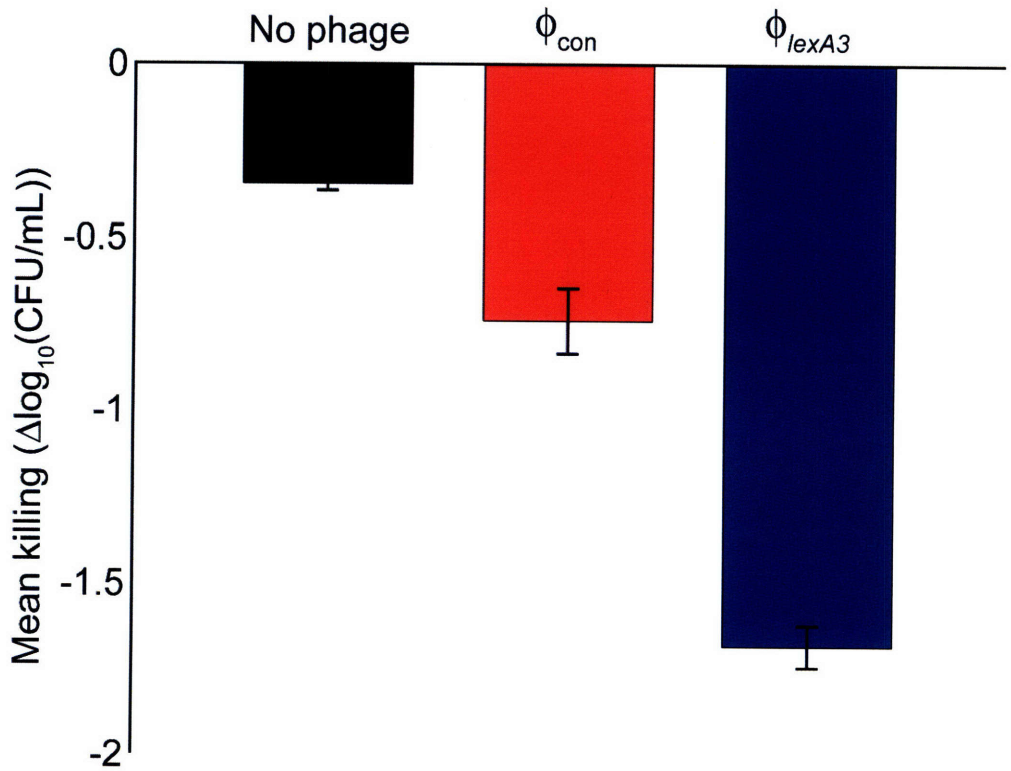

Figure 9. Persister killing assay demonstrates that engineered bacteriophage can be applied to a previously drug-treated population to increase killing of surviving persister cells. After 3 hours of 200 ng/mL ofloxacin treatment,

no phage (black bar), 10^9 PFU/mL unmodified φ_{con} phage (red bar), or 10^9 PFU/mL engineered φ_{lexA3} phage (blue bar) were added to the previously drug-treated cultures. Three additional hours later, viable cell counts were obtained and demonstrated that φ_{lexA3} was able to reduce persister cell levels better than no phage or unmodified φ_{con}.

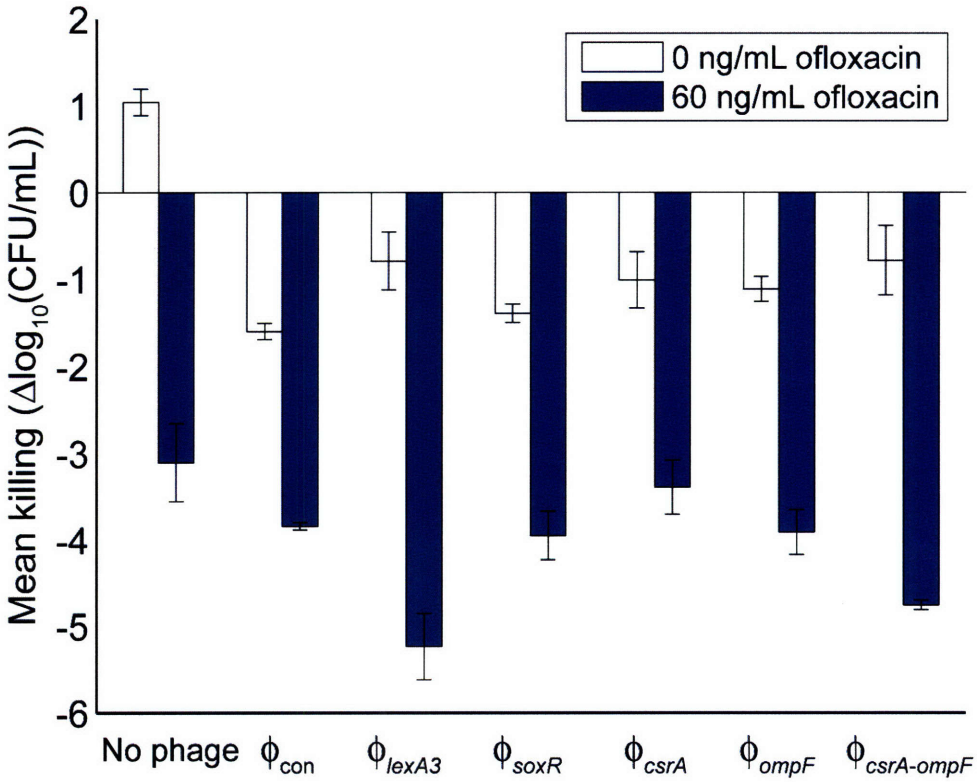

Figure 10. Mean killing with or without 60 ng/mL ofloxacin after 12 hours of treatment of *E. coli* biofilms pregrown for 24 hours. Where indicated, 10^8 PFU/mL of bacteriophage was used. These results demonstrate that φ_{lexA3} and $\varphi_{csrA\text{-}ompF}$ maintain their effectiveness as antibiotic adjuvants against bacteria living in biofilms.

Exposure to subinhibitory concentrations of antibiotics can lead to initial mutations which confer low-level antibiotic resistance and eventually more mutations that yield high-level resistance (101). As effective antibiotic adjuvants, engineered bacteriophage can reduce the number of antibiotic-resistant mutants that result from a bacterial population exposed to antimicrobial drugs. To demonstrate this effect, I grew *E. coli* in media with either no ofloxacin for 24 hours, 30 ng/mL ofloxacin for 24 hours, 30 ng/mL ofloxacin for 12 hours followed by unmodified φ_{con} plus ofloxacin for 12 hours, or 30 ng/mL ofloxacin for 12 hours followed by φ_{lexA3} and ofloxacin for 12 hours (Figure 11). Then, I counted the number of mutants resistant to 100 ng/mL ofloxacin for each of the 60 samples under each growth condition. Growth in the absence of ofloxacin yielded very few resistant cells (median = 1) (Figure 11). However, growth

with subinhibitory levels of ofloxacin produced a very high number of antibiotic-resistant bacteria (median = 1592) (Figure 11). Treatment with unmodified φ_{con} decreased the number of resistant cells moderately (median = 43.5) although all samples contained >1 resistant CFU and over half of the samples had >20 resistant CFUs (Figure 11). In contrast, φ_{lexA3} treatment dramatically suppressed the level of antibiotic-resistant cells (median = 2.5), resulting in a majority of samples with either no resistant CFUs or <20 CFUs (Figure 11).

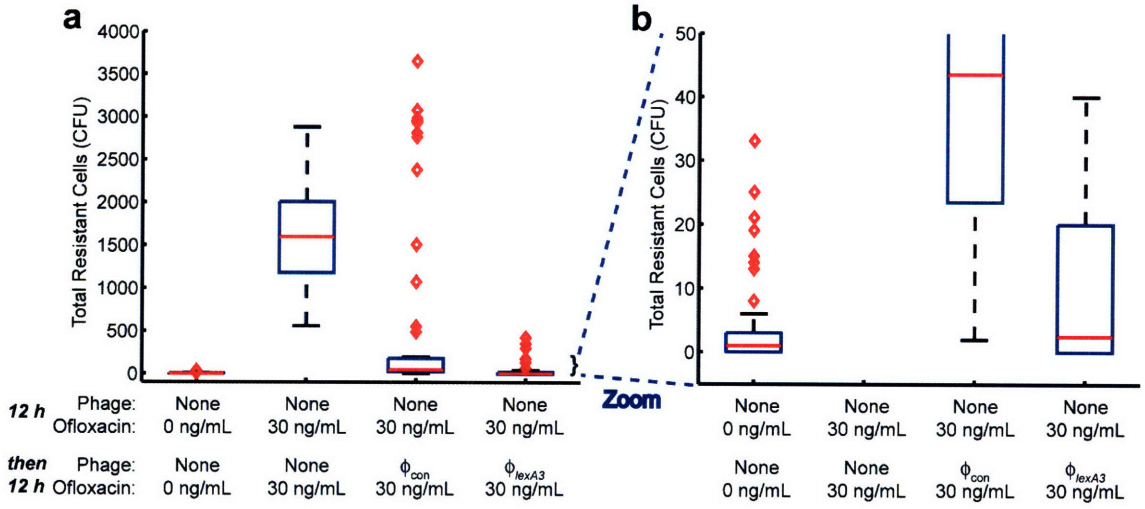

Figure 11. Box-and-whisker plot of the total number of *E. coli* cells in 60 observations that were resistant to 100 ng/mL ofloxacin after growth under various conditions (red bars indicate medians, red diamonds represent outliers). **(a)** Cells grown with no phage and no ofloxacin for 24 hours had very low numbers of antibiotic-resistant cells. Cells grown with no phage and 30 ng/mL ofloxacin for 24 hours had high numbers of resistant cells due to growth in subinhibitory drug concentrations (101). Cells grown with no phage and 30 ng/mL ofloxacin for 12 hours followed by 10^9 PFU/mL unmodified φ_{con} and 30 ng/mL ofloxacin for 12 hours exhibited a modest level of antibiotic-resistant bacteria. Cells grown with no phage and 30 ng/mL ofloxacin for 12 hours followed by 10^9 PFU/mL φ_{lexA3} and 30 ng/mL ofloxacin for 12 hours exhibited a low level of antibiotic-resistant bacteria, close to the numbers seen with no ofloxacin and no phage. **(b)** Zoomed-in version of box-and-whisker plot in **(a)** for increased resolution around low total resistant cell counts confirms that φ_{lexA3} with 30 ng/mL ofloxacin treatment reduced the number of resistant cells to levels similar to that of 0 ng/mL ofloxacin with no phage.

3.2.2 Disrupting the Oxidative Stress Response with SoxR-producing Bacteriophage

To show that other targets could be found, I engineered bacteriophage to express proteins that regulate gene networks or that modulate sensitivity to antibiotics (Figure 6 and Figure 12) (99). For example, the *soxRS* regulon controls a coordinated cellular response to superoxide

(102). SoxR contains a [2Fe-2S] cluster that must be oxidized for it to stimulate SoxS production, which then controls the transcription of downstream genes that respond to oxidative stress (102). Since quinolones generate superoxide-based oxidative attack, I surmised that overproducing wild-type SoxR in bacteriophage (φ_{soxR}) could affect this response and improve ofloxacin's bactericidal activity (Figure 12a) (90, 103). After 6 hours, φ_{soxR} enhanced killing by ofloxacin by 1.9 and 3.8 orders of magnitude compared with unmodified φ_{con} and no phage, respectively (Figure 12b). Interestingly, φ_{soxR} was a better antibiotic adjuvant than bacteriophage producing a SoxR(S95) variant protein which cannot activate SoxS transcription (data not shown) (104). In addition, bacteriophage producing SoxS was not an effective antibiotic adjuvant (data not shown). The discrepancy between SoxR and SoxS overproduction is consistent with previous experiments demonstrating phenotypic differences between Δ*soxR* and Δ*soxS* knockout strains even although activating *soxS* transcription is SoxR's only known function (105). These results suggest that more work is needed to determine the exact mechanisms behind φ_{soxR}'s success as an antibiotic adjuvant. SoxR remains an interesting target since ectopic overexpression of wild-type SoxR has been shown to increase antibiotic susceptibility in cells carrying constitutively-active mutant SoxR proteins (106, 107).

3.2.3 Targeting Multiple Gene Networks with CsrA- and OmpF-producing Bacteriophage

CsrA is a global regulator of glycogen synthesis and catabolism, gluconeogenesis, glycolysis, and biofilm formation (62). Since biofilm formation has been linked to antibiotic resistance, I hypothesized that *csrA*-expressing bacteriophage (φ_{csrA}) might increase susceptibility to antibiotic treatment by affecting gene networks (Figure 12c) (5, 108, 109). In addition, OmpF is a porin which is used by quinolones to enter bacteria (110). Therefore, I surmised that *ompF*-expressing bacteriophage (φ_{ompF}) would increase killing by ofloxacin

(Figure 12c). After 6 hours, both φ_{csrA} and φ_{ompF} increased ofloxacin's bactericidal effect by about 0.8 and 2.7 orders of magnitude compared with unmodified φ_{con} and no phage, respectively (Figure 12d).

To demonstrate the flexibility and effectiveness of engineered bacteriophage as antibiotic adjuvants, I designed an M13mp18 phage to express *csrA* and *ompF* simultaneously ($\varphi_{csrA\text{-}ompF}$) to target *csrA*-controlled gene networks and increase drug penetration (Figure 12c). The combination phage was constructed by placing RBS and *ompF* immediately downstream of *csrA* in φ_{csrA} (Figure 6f) (99). Dual-target $\varphi_{csrA\text{-}ompF}$ was more effective at enhancing ofloxacin's bactericidal effect compared with its single-target relatives, φ_{csrA} and φ_{ompF}, in planktonic (Figure 12d) and biofilm settings (Figure 10). $\varphi_{csrA\text{-}ompF}$ phage performed comparably with φ_{soxR} at various initial phage inoculations (Figure 12e) and at various concentrations of ofloxacin (Figure 12f). Both phages were more effective than no phage or unmodified φ_{con} at increasing killing by ofloxacin. These results demonstrate that engineering bacteriophage to target non-SOS genetic networks and overexpress multiple factors can produce effective antibiotic adjuvants.

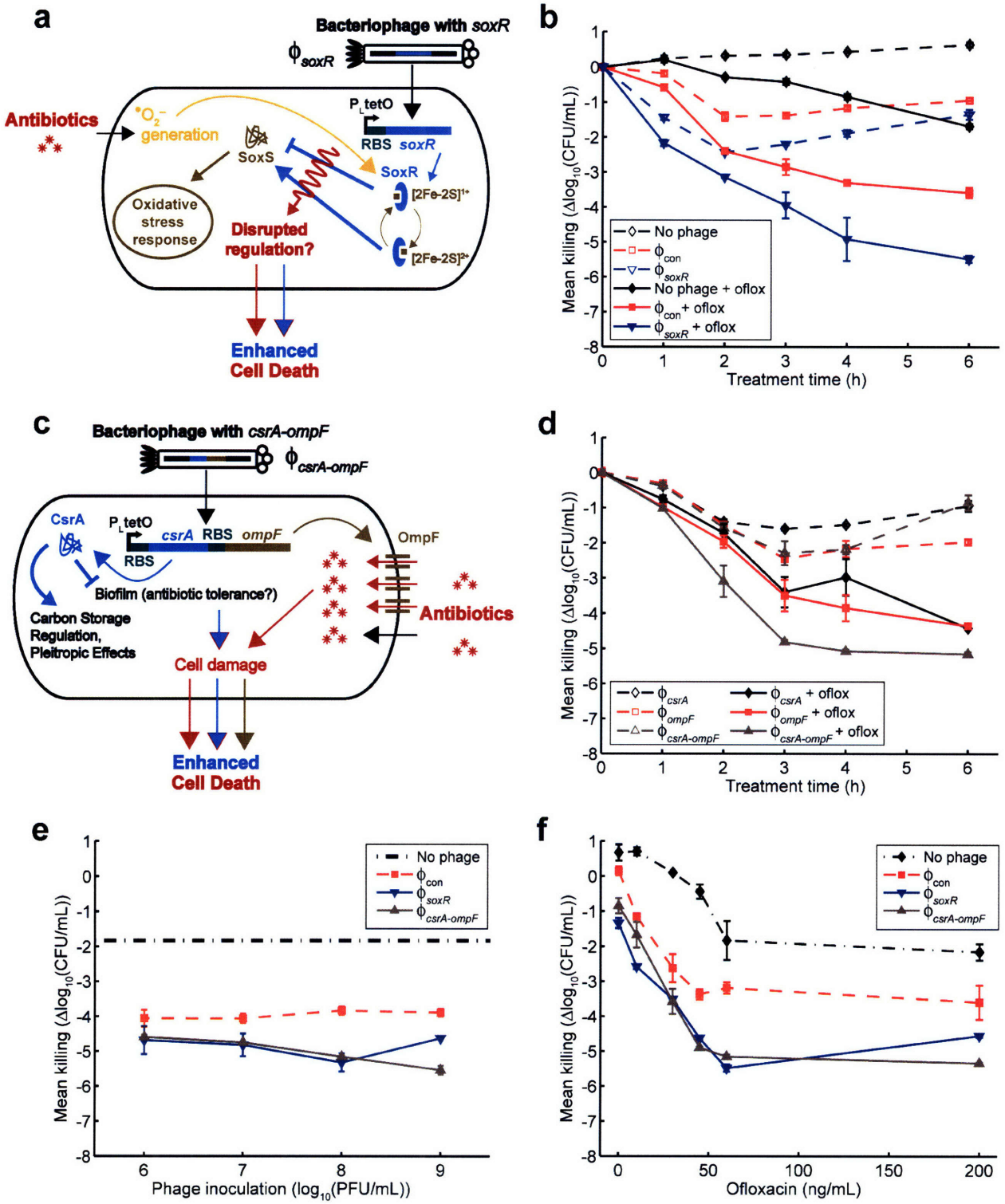

Figure 12. Engineered bacteriophage targeting non-SOS systems as adjuvants for ofloxacin treatment [oflox]. **(a)** Ofloxacin stimulates superoxide generation, which is normally countered by the oxidative stress response, coordinated by SoxR (91). Engineered bacteriophage producing SoxR (φ_{soxR}) enhances ofloxacin-based killing by disrupting regulation of the oxidative stress response. **(b)** Killing curves for no phage (black diamonds), control φ_{con} (red squares), and φ_{soxR} (blue downwards-facing triangles) without ofloxacin (dotted lines, open symbols) or with 60 ng/mL ofloxacin (solid lines, closed symbols). 10^8 PFU/mL phage was used. Killing curves for no phage and unmodified φ_{con} are reproduced from **Figure 8b** for comparison and show that φ_{soxR} enhances killing by ofloxacin.

(c) CsrA suppresses the biofilm state in which bacterial cells tend to be more resistant to antibiotics (62). OmpF is a porin used by quinolones to enter into bacterial cells (110). Engineered bacteriophage producing both CsrA and OmpF simultaneously ($\varphi_{csrA\text{-}ompF}$) represses biofilm formation and antibiotic tolerance via CsrA and enhances antibiotic penetration via OmpF to produce an improved dual-targeting adjuvant for ofloxacin. **(d)** Killing curves for φ_{csrA} (black diamonds), φ_{ompF} (red squares), and $\varphi_{csrA\text{-}ompF}$ (brown upwards-facing triangles) without ofloxacin (dotted lines, open symbols) or with 60 ng/mL ofloxacin (solid lines, closed symbols). 10^8 PFU/mL phage was used. Phage expressing both *csrA* and *ompF* ($\varphi_{csrA\text{-}ompF}$) is a better adjuvant for ofloxacin than phage expressing *csrA* alone (φ_{csrA}) or *ompF* alone (φ_{ompF}). **(e)** Phage dose response shows that both φ_{soxR} (blue downwards-facing triangles with solid line) and $\varphi_{csrA\text{-}ompF}$ (brown upwards-facing triangles with solid line) are effective as adjuvants for ofloxacin (60 ng/mL) over a wide range of initial inoculations. Phage dose response curves for no phage (black dash-dotted line) and unmodified φ_{con} (red squares with dashed line) are reproduced from **Figure 8c** for comparison. **(f)** Ofloxacin dose response shows that both φ_{soxR} (blue downwards-facing triangles with solid line) and $\varphi_{csrA\text{-}ompF}$ (brown upwards-facing triangles with solid line) improve killing throughout a range of drug concentrations. 10^8 PFU/mL phage was used. Ofloxacin dose response curves for no phage (black diamonds with dash-dotted line) and unmodified φ_{con} (red squares with dashed line) are reproduced from **Figure 8d** for comparison.

3.3 Discussion

I have demonstrated that effective bacteriophage adjuvants which target different factors individually or in combination can be built in a modular fashion. To extend our work, libraries of existing phage could be modified to target gene networks, such as the SOS response, in different bacterial species (66, 67). With current DNA sequencing and synthesis technology, an entire engineered M13mp18 genome carrying multiple constructs to target genetic networks could be synthesized for less than $10,000, a price which is sure to decrease in the future, enabling large-scale modifications of phage libraries (37, 39, 65, 111). Furthermore, systems biology could be employed to rapidly identify new targets (90, 91). For example, targets that confer increased antibiotic susceptibility could be identified using large-scale screening with the ASKA overexpression library and rapidly moved into bacteriophage to create new antimicrobial adjuvants (112). Cocktails of engineered phage such as those described here could be combined with biofilm-dispersing bacteriophage and antibiotics to increase the removal of harmful biofilms (42). Antisense RNA (asRNA) could also be delivered by bacteriophage to enhance killing of bacteria. For example, I have constructed plasmids with *recA*-asRNA, *recB*-asRNA, and *recC*-asRNA as well as all pairwise *recA*, *recB*, and *recC* combinations and assayed for persistence levels with ofloxacin (5 μg/mL) with 8 hours of growth followed by 8 hours of

treatment. The strongest phenotypes observed were with the $P_L$tetO-*recB*-asRNA/$P_L$lacO-*recA*-asRNA and $P_L$tetO-*recC*-asRNA/$P_L$lacO-*recB*-asRNA plasmids. These constructs displayed 1.87 and 2.37 $\log_{10}$(CFU/mL) less persisters, respectively, compared with wild-type *E. coli* EMG2. These constructs displayed 0.97 and 1.47 $\log_{10}$(CFU/mL) less persisters, respectively, compared with a control plasmid described in Section 4 (pZE21s1-*cat*) (Figure 16). These asRNA constructs could potentially be useful in suppressing the SOS response if delivered by bacteriophage.

Despite the potential benefits described above, phage therapy has yet to be accepted into clinical practice because few clinical trials have been conducted (28). Issues with phage therapy such as phage immunogenicity, efficacy, target bacteria identification and phage selection, host specificity, and toxin release must be addressed in clinical studies and shown to be surmountable (11, 30-33). I believe that engineered phage would be more readily adopted in industrial, agricultural, and food processing settings where bacterial biofilms and other difficult-to-clear bacteria are present (27, 42). Applying bacteriophage as antibiotic adjuvants in non-medical settings should be economically advantageous, reduce community-acquired antibiotic resistance, and be a prudent first step towards gaining acceptance for clinical use (19).

A crucial component of using engineered bacteriophage to target gene networks to produce powerful antibiotic adjuvants is to take advantage of the numerous autoregulated repressors inherent in bacteria that regulate resistance genes or cell repair pathways (113). For example, I used *lexA* in engineered bacteriophage since it represses the SOS response until it is cleaved by *recA* in response to DNA damage (90). Other repressors include *marR*, which represses the *marRAB* operon, and *acrR*, which represses the *acrAB* operon; both operons confer resistance to a range of antibiotics (113). Simple overexpression of these repressors can decrease the activity

of the SOS response or antibiotic-resistance-conferring operons. However, simple overexpression may impose a high metabolic cost on the cells leading to rejection of the introduced constructs. An alternative strategy is to create autoregulated negative-feedback modules with *lexA* and other repressors (Figure 13). The net effect of this strategy should be to increase the loop gain of inherent autoregulated negative-feedback loops so that any perturbations in the level of repressors will be more rapidly restored, hopefully preventing successful activation of survival pathways. For example, I have produced and tested the pZE1L-*lexA* plasmid for persistence levels with ofloxacin (5 μg/mL) with 8 hours of growth followed by 8 hours of treatment (Figure 13). Cells containing the pZE1L-*lexA* construct produced about 1.44 $\log_{10}$(CFU/mL) less persisters compared with wild-type *E. coli* EMG2. The $P_L$lexO-RBS-*lexA* construct could be migrated to bacteriophage using the techniques described above.

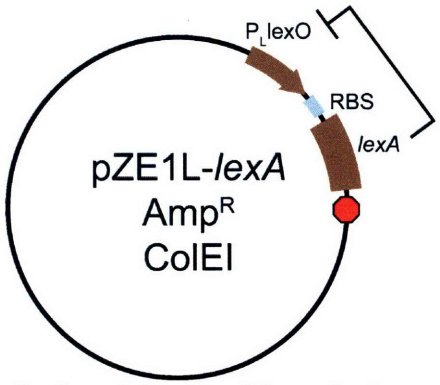

Figure 13. Autoregulated negative-feedback module with wild-type *lexA* repressing $P_L$lexO from Ref. (86) may increase the level of *lexA* expression when *lexA* is cleaved by recA in response to DNA damage by agents such as ofloxacin.

Conventional drugs typically achieve their therapeutic effect by reducing protein function. In contrast, the approach I have described here enhances killing by antibiotics by overproducing proteins that affect gene networks, such as LexA3, SoxR, and CsrA, or that act on their own to modulate antibiotic sensitivity, such as OmpF. These gene networks could also be targeted by non-phage delivery mechanisms including mobile genetic elements and chemical-based drug

delivery. Combination therapy with antibiotics and engineered phage resulted in strong bactericidal action and no noticeable development of phage resistance. Our work demonstrates that targeting genetic networks in bacteria which are not primary antibiotic targets can yield substantial improvements in killing by antimicrobial drugs. Advances in systems biology and synthetic biology should enable the practical application of engineered bacteriophage with antibiotics as new combination treatments for combating bacterial infections.

3.4 Materials and Methods

3.4.1 Bacterial strains, bacteriophage, and chemicals.

E. coli wild-type EMG2 cells were obtained from the Yale Coli Genetic Stock Center (CGSC #4401). M13mp18 bacteriophage was purchased from New England Biolabs, Inc. (Ipswich, MA). *E. coli* XL-10 cells used for cloning, amplifying phage, and plating phage were obtained from Stratagene (La Jolla, CA).

T4 DNA ligase and all restriction enzymes were purchased from New England Biolabs, Inc. (Ipswich, MA). PCR reactions were carried out using PCR SuperMix High Fidelity from Invitrogen (Carlsbad, CA) or Phusion High Fidelity from New England Biolabs, Inc. (Ipswich, MA). Purification of PCR reactions and restriction digests was carried out with the QIAquick Gel Extraction or PCR Purification kits (Qiagen, Valencia, CA). Plasmid DNA was isolated using the QIAprep Spin Miniprep kit (Qiagen, Valencia, CA). All other chemicals and materials were purchased from Fisher Scientific, Inc. (Hampton, NH).

3.4.2 Engineering M13mp18 bacteriophage to target genetic networks.

To construct engineered phage, *lexA3*, *soxR*, *csrA*, and *ompF* genes were first placed under the control of the $P_L$tetO promoter in the pZE11G vector (99, 100). Using PCR with primers 5'

ttatca ggtacc atgAAAGCGT TAACGGCC 3' and 5' atacat aagctt TTACAGCCA GTCGCCG 3', *lexA3* was cloned between the KpnI and HindIII sites of pZE11G to form pZE11-*lexA3*. Since *soxR* has an internal KpnI site, I built a synthetic RBS by sequential PCR using 5' agaggagaaa ggtacc atgGAAAAGA AATTACCCCG 3' and 5' atacat aagctt TTAGT TTTGTTCATC TTCCAG 3' followed by 5' agtaga gaattc attaaagaggagaaa ggtacc atg 3' and 5' atacat aagctt TTAGT TTTGTTCATC TTCCAG 3'. The resulting EcoRI-RBS-*soxR*-HindIII DNA was ligated to an XhoI-$P_L$tetO-EcoRI fragment excised from pZE11G and the entire DNA fragment was ligated into pZE11G between XhoI and HindIII to form pZE11-*soxR* (99). Primers for *csrA* for cloning into pZE11G in between KpnI and HindIII to form pZE11-*csrA* were 5' agaggagaaa ggtacc atgCTGATTC TGACTCGT 3' and 5' atacat aagctt TTAGTA ACTGGACTGC TGG 3'; and for *ompF* to form pZE11-*ompF*, 5' agaggagaaa ggtacc atgATGAAGC GCAATATTCT 3' and 5' atacat aagctt TTAGAACTG GTAAACGATA CC 3'. To express *csrA* and *ompF* simultaneously under the control of $P_L$tetO, I PCR amplified RBS-*ompF* DNA from pZE11-*ompF* using 5' ccagtc aagctt attaaagaggagaaa ggtacc 3' and 5' atacat GGATCC TTAGAACTG GTAAACGATA CC 3' and cloned the product in between HindIII and BamHI in pZE11-*csrA* to form pZE11-*csrA-ompF*. The resulting plasmids were transformed into *E. coli* XL-10 cells.

All $P_L$tetO-gene constructs followed by terminator T1 of the *rrnB* operon and preceded by a stop codon were PCR amplified from the respective pZE11 plasmids with primers 5' aataca GAGCTC cTAA tccctatcagtgatagagattg 3' and 5' taatct CGATCG tctagggcggcggat 3' and cloned into the SacI and PvuI sites of M13mp18 (Figure 6) (96, 99, 100). Resulting phage genomes were transformed into XL-10 cells, mixed with 200 μL overnight XL-10 cells in 3 mL top agar, 1 mM IPTG, and 40 μL of 20 mg/mL X-gal, and poured onto LB agar + chloramphenicol (30 μg/mL) plates for plaque formation and blue-white screening. After

overnight incubation of plates at 37°C, white plaques were scraped and placed into 1:10 dilutions of overnight XL-10 cells and grown for 5 hours. Replicative form (RF) M13mp18 DNA was collected by DNA minipreps of the bacterial cultures. All insertions into M13mp18 were verified by PCR and restriction digests of RF DNA. Infective bacteriophage solutions were obtained by centrifuging infected cultures for 5 minutes at 16,100 x *g* and collecting supernatants followed by filtration through Nalgene #190-2520 0.2 μm filters (Nalge Nunc International, Rochester, NY).

3.4.3 Determination of plaque forming units.

To obtain plaque forming units, I added serial dilutions of bacteriophage performed in 1x PBS to 200 μL of overnight XL-10 cells in 3 mL top agar, 1 mM IPTG, and 40 μL of 20 mg/mL X-gal, and poured the mixture onto LB agar + chloramphenicol (30 μg/mL) plates. After overnight incubation at 37°C, plaques were counted.

3.4.4 Determination of colony forming units.

To obtain CFU counts, 150 μL of relevant cultures were collected, washed with 1x phosphate-buffered saline (PBS), recollected, and resuspended in 150 μL of 1x PBS. Serial dilutions were performed with 1x PBS and sampled on LB agar plates. LB agar plates were incubated at 37°C overnight before counting.

3.4.5 Flow cytometer assay of SOS induction.

To monitor φ_{lexA3}'s suppression of the SOS response (Figure 7), I used a plasmid containing an SOS-response promoter driving *gfp* expression in EMG2 cells ($P_L$lexO-*gfp*) (90). After growing 1:500 dilutions of the overnight cells for 2 hours and 15 minutes at 37°C and 300 rpm (model G25 incubator shaker, New Brunswick Scientific), I applied ofloxacin and

bacteriophage and treated for 6 hours at 37°C and 300 rpm. Cells were then analyzed for GFP fluorescence using a Becton Dickinson (Franklin Lakes, NJ) FACScalibur flow cytometer with a 488-nm argon laser and a 515-545 nm emission filter (FL1) at low flow rate. The following photo-multiplier tube (PMT) settings were used for analysis: E00 (FSC), 275 (SSC), and 700 (FL1). Becton Dickinson Calibrite Beads were used for instrument calibration. 200,000 cells were collected for each sample and processed with MATLAB (Mathworks, Natick, MA).

3.4.6 Ofloxacin killing assay.

To determine the adjuvant effect of engineered phage (Figure 8b, Figure 12b, and Figure 12d), I grew 1:500 dilutions of overnight EMG2 cells for 3 hours and 30 minutes at 37°C and 300 rpm to late-exponential phase and determined initial CFUs. Then, I added 60 ng/mL ofloxacin by itself or in combination with 10^8 PFU/mL bacteriophage (unmodified φ_{con} phage or engineered M13mp18 phage) and treated at 37°C and 300 rpm. At indicated time points, I determined CFUs as described above. Mean killing ($\Delta\log_{10}$(CFU/mL)) was determined by subtracting mean initial $\log_{10}$(CFU/mL) from mean $\log_{10}$(CFU/mL) after treatment in order to compare data from different experiments. In addition, viable cell counts were obtained for ofloxacin-free EMG2 cultures, ofloxacin-free EMG2 cultures with φ_{con} control phage, and ofloxacin-free EMG2 cultures with engineered phage.

3.4.7 Dose response assays.

The initial phage inoculation dose response experiments (Figure 8c and Figure 12e) were handled using the same protocol as the ofloxacin killing assay except that 60 ng/mL ofloxacin was added with varying concentrations of phage. Cultures were treated for 6 hours before obtaining viable cell counts. The ofloxacin dose response experiments (Figure 8d and Figure 12f) were also obtained using the same protocol as the ofloxacin killing assay except that 10^8

PFU/mL phage was added with varying concentrations of ofloxacin and viable cell counts were obtained after 6 hours of treatment.

3.4.8 Gentamicin and ampicillin killing assays.

To determine the adjuvant effect of engineered bacteriophage for gentamicin and ampicillin, I used the same protocol as the ofloxacin killing assay except that I used 10^9 PFU/mL initial phage inoculations. 5 μg/mL gentamicin and 5 μg/mL ampicillin were used in Figure 8e and Figure 8f, respectively.

3.4.9 Persister killing assay.

I performed a persister killing assay to determine whether engineered phage could help to kill persister cells in a population which survived initial drug treatment without bacteriophage (Figure 9). I first grew 1:500 dilutions of overnight EMG2 for 3 hours and 30 minutes at 37°C and 300 rpm followed by treatment with 200 ng/mL ofloxacin for 3 hours to create a population of surviving bacteria. Then, I added either no phage, 10^9 PFU/mL control φ_{con} phage, or 10^9 PFU/mL engineered φ_{lexA3} phage. After 3 hours of additional treatment, I collected the samples and assayed for viable cell counts as described above.

3.4.10 Biofilm resistance assay.

Biofilms were grown using E. coli EMG2 cells according to a previously-reported protocol (42). Briefly, lids containing plastic pegs (MBEC Physiology and Genetics Assay, Edmonton, CA) were placed in 96-well plates containing overnight cells that were diluted 1:200 in 150 μL LB. Plates were then inserted into plastic bags to minimize evaporation and inserted in a Minitron shaker (Infors HT, Bottmingen, Switzerland). After 24 hours of growth at 35°C and 150 rpm, lids were moved into new 96-well plates with 200 μL LB with or without 10^8 PFU/mL

of bacteriophage. After 12 hours of treatment at 35°C and 150 rpm, lids were removed, washed three times in 200 μL of 1x PBS, inserted into Nunc #262162 microtiter plates with 150 μL 1x PBS, and sonicated in an Ultrasonics 5510 sonic water bath (Branson, Danbury, CT) at 40 kHz for 30 minutes. Serial dilutions, using the resulting 150 μL 1x PBS, were performed on LB plates and viable cell counts were determined. Mean killing ($\Delta\log_{10}$(CFU/mL)) was calculated by subtracting mean $\log_{10}$(CFU/mL) after 24 hours of growth from mean $\log_{10}$(CFU/mL) after 12 hours of treatment (Figure 10).

3.4.11 Antibiotic resistance assay.

To analyze the effect of subinhibitory concentrations of ofloxacin on the development of antibiotic-resistant mutants, I grew $1{:}10^8$ dilutions of overnight EMG2 in LB media containing either no ofloxacin or 30 ng/mL ofloxacin (Figure 11). After 12 hours of growth at 37°C and 300 rpm, I split the cells grown in no ofloxacin into 100 μL aliquots with no ofloxacin in 60 wells in 96-well plate format (Costar 3370; Fisher Scientific, Pittsburgh, PA). I also split the cells grown in 30 ng/mL ofloxacin into 100 μL aliquots in 60 wells with either no phage and 30 ng/mL ofloxacin, φ_{con} and 30 ng/mL ofloxacin, and φ_{lexA3} and 30 ng/mL ofloxacin in 96-well plate format. I placed the 96-well plates in 37°C and 300 rpm with plastic bags to minimize evaporation. After 12 hours of treatment, I plated cultures from each well on LB agar + 100 ng/mL ofloxacin to select for mutants that developed resistance against ofloxacin. To compare results, I constructed box-and-whisker plots using the 60 individual observations for each treatment condition (Figure 11).

3.4.12 Statistical analysis.

All CFU data were $\log_{10}$-transformed prior to analysis. For all data points in all experiments, $n = 3$ samples were collected except where noted. Error bars in figures indicate standard error of the mean.

4 *IN VIVO* SENSORS FOR ANTIBIOTIC RESISTANCE GENES

4.1 Introduction

Antibacterial drugs currently available do not reduce the fundamental evolutionary pressures that underlie the development of antibiotic resistance. To address this problem head-on, I developed a system to enable the selective killing of antibiotic-resistant bacteria and reducing the spread of resistance genes. Such a system utilizes two-component synthetic gene circuits to first detect antibiotic-resistance genes *in vivo* (the sensor component) and subsequently activate killing pathways, repress horizontal transmission in those cells, or express a reporter like GFP (the effector component). The critical component in this system is the sensor since it must be accurate and sensitive *in vivo* in order to correctly signal the effector component, which is comparatively easy to design since it is most likely to involve overexpression of a protein. To build the sensor component, I designed a synthetic sensor to detect antibiotic-resistance mRNAs. I took advantage of competitive inhibition with antisense RNA to build a system that will give a high output level when the mRNA species to be detected is present and a low output level when it is absent. I developed and tested *in vivo* sensor designs utilizing antisense RNA to detect mRNA *in vivo*. The ability produce an output when a particular mRNA is present allows the detection of cells that carry genes which confer antibiotic resistance or the building of a kill-switch that eliminates cells carrying antibiotic resistance genes in a population.

These gene circuits were built using both antisense RNA and proteins and can be flexibly applied to different antibiotic-resistance genes using nucleic acid synthesis technologies. For example, an *in vivo* sensor can detect the presence of the choramphenicol-acetyltransferase gene (*cat*) inside an individual cell and activate an effector circuit to kill the bacteria. Such a circuit can be used to reduce the number of antibiotic-resistant bacteria in a population without exerting

evolutionary pressure on non-resistant cells. This system can also be used to reduce the spread of resistance genes or used simply as an *in vivo* detector. Antibiotics can mobilize antibiotic-resistance genes by causing cleavage of repressor proteins which normally suppress horizontal transmission. A synthetic gene circuit designed to have the repressor protein suppress its own production will result in the overexpression of the repressor in cases where it is cleaved due to antibiotic therapy. Therefore, by maintaining high levels of the repressor, horizontal transmission of antibiotic-resistance genes can be significantly reduced. In the absence of antibiotics, the synthetic gene circuit will remain dormant and thus will not impose evolutionary fitness disadvantages. These synthetic gene circuits can be delivered to bacteria via chemical drug delivery, the bacteriophage platform described above, or mobile genetic elements, such as those used by antibiotic-resistance genes themselves, in a "Trojan horse" style attack. This system can be used in combination with the bacteriophage described in Section 3 to dramatically enhance bacterial killing and minimize the incidence of antibiotic-resistant bacteria. Whereas engineered bacteriophage targeting gene networks (Section 3) are primarily useful in preventing the development of antibiotic resistance, this system can reduce the level of antibiotic resistance in a population and prevent its spread. As a result, this system can be applied to patients or in livestock who are known to carry resistant bacteria in order to restore antibiotic susceptibility and decrease hospital-acquired and community-acquired antibiotic resistance. Thus, this system presents a practical way to directly and selectively combat the mechanisms underlying antibiotic resistance.

4.2 Design and Results

4.2.1 Design 1: pZE21s1-*cat*

The first design extends the paired-termini (PT7) design described in Ref. (114) which produces an antisense RNA similar to that shown in Figure 14. The PT7 construct produces antisense RNA with longer half-lives *in vivo*, allowing for greater antisense effect (114). Starting with the PT7 construct shown in Figure 14, the NcoI and XhoI sites were replaced by HindIII and NheI sites, respectively.

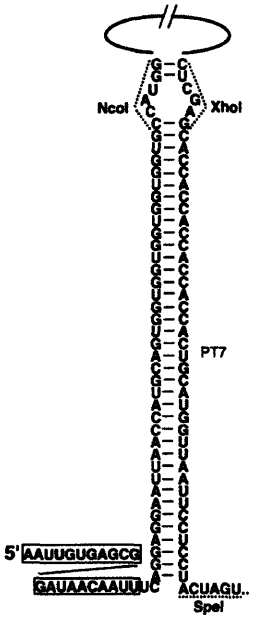

Figure 14. Paired-termini design from Ref. (114) in which the antisense RNA is cloned between the flanking restriction sites at the top of the stem. Reprinted from Ref. (114).

I chose to target *cat* since it represents a very well-characterized and important gene in *E. coli* encoding chloramphenicol resistance (115). Using the paired-termini (PT) asRNA system (114), I designed antisense RNA to target *cat* mRNA primarily in the 5'-untranslated region, the RBS region, and the 5' end of the coding region (from the *cat* transcriptional start site to base pair 300 in the *cat* gene) (114). DNA encoding antisense RNA to an antibiotic resistance gene target such as chloramphenicol acetyltransferase (*cat*, conferring chloramphenicol resistance

(Cm^R) was cloned in between HindIII and NheI sites near the top of the stem of the PT7 construct. The resulting PT7-*cat*-asRNA construct produces an antisense RNA that can bind to *cat* RNA and repress *cat* expression (Figure 15). I cloned PT7-*cat*-asRNA under the inducible control of anhydrotetracycline (aTc) by using pZE21Y12α12GFP (99, 116), taking care to remove the *cis*-repressive sequence and GFP. In order to design a plasmid that can detect the presence of target *cat* mRNA, I fused the *cat* gene with the *gfp* gene to produce a construct (*cat-gfp*) that is inhibited by PT7-*cat*-asRNA and thus produces low GFP levels normally. I did this by fusing a portion of *cat* DNA that encodes the 5'-untranslated region, the RBS, and the 5' end of the coding region to *gfp* at a NotI restriction site. In this design, the *cat-gfp* fusion acts as the effector component (here, the effector is merely a reporter) while the PT7-*cat*-asRNA acts as the sensor component (Table 1). The *cat-gfp* fusion was then placed under the control of P_{BAD} in the same vector as the sensor. The resulting sensor-reporter plasmid (pZE21s1-*cat*) was cloned into E. coli DH5αPro cells by itself or with a plasmid that either carried *cat* (pZA3) or *bla* (pZA1) (Figure 16). pZA3 and pZA1 were both constructed from plasmids described in Ref. (99) with the synthetic promoters and genes removed by deleting all DNA between the XhoI and XmaI restriction sites.

Table 1. Sequence of pZE21s1-*cat* plasmid. PT7 antisense stem loop structure is highlighted in yellow (114). DNA coding for antisense RNA to *cat* is highlighted in red. DNA sequence for *cat-gfp* fusion is shown in grey and green text, respectively.

ctcgag
tccctatcagtgatagagattgacatccctatcagtgatagagatactgagcacatcagcaggacgcactgacc
gaattc
AGGAGGAATT AACCATGCAG TGGTGGTGGT GGTGGTG
AAGCTT
TATAGGTACATTGAGCAACTGACTGAAATGCCTCAAAATGTTCTTTACGATGCCATTGGGATATATCAACGGTGGTA
TATCCAGTGATTTTTTTCTCCATTTTAGCTTCCTTAGCTCCTGAAAATCTCGATAACTCAAAAAATACGCCCGGTAG
TGATC
GCTAGC
CACCACC ACCACCACCA CTGCATGGTT AATTCCTCCT
cccggg
ggatcc

catggt
acgcgt
ggcatcaaataaaacgaaaggctcagtcgaaagactgggcctttcgtttt
atctgttgtttgtcggtgaacgctctcctgagtaggacaaatccgccgccctaga
cctagg
cgttcggctgcggcgagcggtatcagctcactcaaaggcggtaatacggttatccacagaatcaggggataacgcag
gaaagaacatgtgagcaaaaggccagcaaaaggccaggaaccgtaaaaaggccgcgttgctggcgtttttccatagg
ctccgccccccctgacgagcatcacaaaaatcgacgctcaagtcagaggtggcgaaacccgacaggactataaagata
ccaggcgtttccccctggaagctccctcgtgcgctctcctgttccgaccctgccgcttaccggatacctgtccgcct
ttctcccttcgggaagcgtggcgctttctcaatgctcacgctgtaggtatctcagttcggtgtaggtcgttcgctcc
aagctgggctgtgtgcacgaaccccccgttcagcccgaccgctgcgccttatccggtaactatcgtcttgagtccaa
cccggtaagacacgacttatcgccactggcagcagccactggtaacaggattagcagagcgaggtatgtaggcggtg
ctacagagttcttgaagtggtggcctaactacggctacactagaaggacagtatttggtatctgcgctctgctgaag
ccagttaccttcggaaaaagagttggtagctcttgatccggcaaacaaaccaccgctggtagcggtggttttttgt
ttgcaagcagcagattacgcgcagaaaaaaaggatctcaagaagatcctttgatcttttctacggggtctgacgctc
agtggaacgaaaactcacgttaagggattttggtcatg
actagt
gcttggattctcaccaataaaaaacgcccggcggcaaccgagcgttctgaac
aaatccagatggagttctgaggtcattactggatctatcaacaggagtccaagc
gagctc
tcgaaccccagagtcccgctcagaagaactcgtcaagaaggcgatagaaggcgatgcgctgcgaatcgggagcggcg
ataccgtaaagcacgaggaagcggtcagcccattcgccgccaagctcttcagcaatatcacgggtagccaacgctat
gtcctgatagcggtccgccacacccagccggccacagtcgatgaatccagaaaagcggccattttccaccatgatat
tcggcaagcaggcatcgccatgggtcacgacgagatcctcgccgtcgggcatgcgcgccttgagcctggcgaacagt
tcggctggcgcgagcccctgatgctcttcgtccagatcatcctgatcgacaagaccggcttccatccgagtacgtgc
tcgctcgatgcgatgtttcgcttggtggtcgaatgggcaggtagccggatcaagcgtatgcagccgccgcattgcat
cagccatgatggatactttctcggcaggagcaaggtgagatgacaggagatcctgccccggcacttcgcccaatagc
agccagtcccttcccgcttcagtgacaacgtcgagcacagctgcgcaaggaacgcccgtcgtggccagccacgatag
ccgcgctgcctcgtcctgcagttcattcagggcaccggacaggtcggtcttgacaaaaagaaccgggcgcccctgcg
ctgacagccggaacacggcggcatcagagcagccgattgtctgttgtgcccagtcatagccgaatagcctctccacc
caagcggccggagaacctgcgtgcaatccatcttgttcaatcatgcgaaacgatcctcatcctgtctcttgatcaga
tcttgatcccctgcgccatcagatccttggcggcaagaaagccatccagtttactttgcagggcttcccaaccttac
cagagggcgccccagctggcaattcc
GACGTC
TTT
GGGCCC
AAGGCCCAGTCTTTCGACTGAGCCTTTCGTTTTATTTGATGCCTGGCAGTTCCCTACTCTCGCATGGGGAGACCCCA
CACTACCATCGGCGCTACGGCGTTTCACTTCTGAGTTCGGCATGGGGTCAGGTGGGACCACCGCGCTACTGCCGCCA
GGCAAATTCTGTT
TCTAGA
TTATTTGTATAGTTCATCCATGCCATGTGTAATCCCAGCAGCTGTTACAAACTCAAGAAGGACCATGTGGTCTCTCT
TTTCGTTGGGATCTTTCGAAAGGGCAGATTGTGTGGACAGGTAATGGTTGTCTGGTAAAAGGACAGGGCCATCGCCA
ATTGGAGTATTTTGTTGATAATGGTCTGCTAGTTGAACGCTTCCATCTTCAATGTTGTGTCTAATTTTGAAGTTAAC
TTTGATTCCATTCTTTTGTTTGTCTGCCATGATGTATACATTGTGTGAGTTATAGTTGTATTCCAATTTGTGTCCAA
GAATGTTTCCATCTTCTTTAAAATCAATACCTTTTAACTCGATTCTATTAACAAGGGTATCACCTTCAAACTTGACT
TCAGCACGTGTCTTGTAGTTCCCGTCATCTTTGAAAAATATAGTTCTTTCCTGTACATAACCTTCGGGCATGGCACT
CTTGAAAAAGTCATGCTGTTTCATATGATCTGGGTATCTCGCAAAGCATTGAACACCATAACCGAAAGTAGTGACAA
GTGTTGGCCATGGAACAGGTAGTTTTCCAGTAGTGCAAATAAATTTAAGGGTAAGTTTTCCGTATGTTGCATCACCT
TCACCCTCTCCACTGACAGAAAATTTGTGCCCATTAACATCACCATCTAATTCAACAAGAATTGGGACAACTCCAGT
GAAAAGTTCTTCTCCTTTACG
C GCGGCCGC
cgccccgccctgccactcatcgcagtactgttgtaattcattaagcattctgccgacatggaagccatcacagacgg
catgatgaacctgaatcgccagcggcatcagcaccttgtcgccttgcgtataatatttgcccatggtgaaaacgggg
gcgaagaagttgtccatattggccacgtttaaatcaaaactggtgaaactcacccagggattggctgagacgaaaaa
catattctcaataaaccctttagggaaataggccaggttttcaccgtaacacgccacatcttgcgaatatatgtgta
gaaactgccggaaatcgtcgtggtattcactccagagcgatgaaaacgtttcagtttgctcatggaaaacggtgtaa
caagggtgaacactatcccatatcaccagctcaccgtctttcattgccatacggaattccggatgagcattcatcag

gcgggcaagaatgtgaataaaggccggataaaacttgtgcttatttttctttacggtctttaaaaaggccgtaatat
ccagctgaacggtctggttataggtacattgagcaactgactgaaatgcctcaaaatgttctttacgatgccattgg
gatatatcaacggtggtatatccagtgatttttttctccattttagcttccttagctcctgaaaatctcgataactc
aaaaaatacgcccggtagtgatc
GTCGAC
TATGGAGAAACAGTAGAGAGTTGCGATAAAAAGCGTCAGGTAGGATCCGCTAATCTTATGGATAAAAATGCTATGGC
ATAGCAAAGTGTGACGCCGTGCAAATAATCAATGTGGACTTTTCTGCCGTGATTATAGACACTTTTGTTACGCGTTT
TTGTCATGGCTTTGGTCCCGCTTTGTTACAGAATGCTTTTAATAAGCGGGGTTACCGGTTTGGTTAGCGAGAAGAGC
CAGTAAAAGACGCAGTGACGGCAATGTCTGATGCAATATGGACAATTGGTTTCTT

If an external source of *cat* is present, *cat* mRNA should compete with *cat-gfp* mRNA for binding to PT7-*cat*-asRNA (Figure 15). As a result, repression of the *cat-gfp* fusion should be reduced, resulting in greater GFP expression (Figure 15). Thus, this sensor design (pZE21s1-*cat*) should yield higher GFP levels in the presence of a *cat*-containing plasmid (pZA3) as compared to a non-*cat*-containing plasmid (pZA1) (Figure 16).

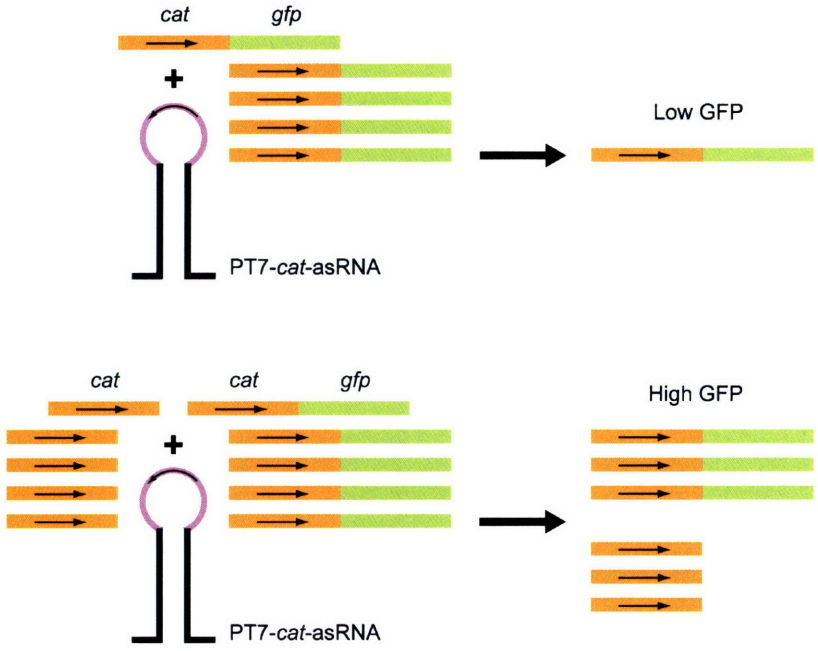

Figure 15. RNA sensor design #1 should repress the *cat-gfp* fusion in the absence of a *cat*-containing plasmid such as pZA3, leading to low GFP output. In the presence of pZA3, *cat* mRNA should compete with *cat-gfp* mRNA for PT7-*cat*-asRNA, leading to derepression of *cat-gfp* and thus higher GFP output.

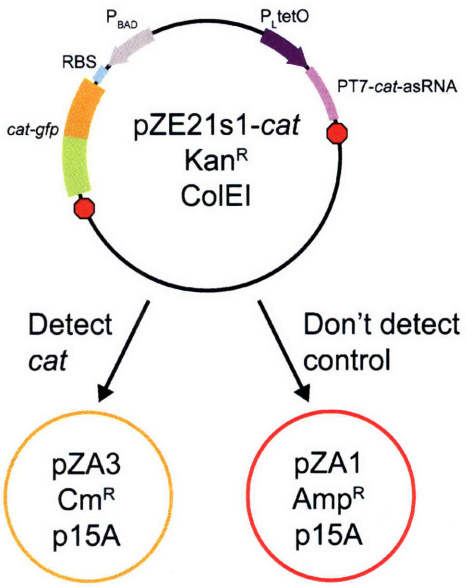

Figure 16. RNA sensor design #1 (pZE21s1-*cat*) should detect a *cat*-containing plasmid such as pZA3 and not a *bla*-containing Amp^R plasmid such as pZA1. Kan^R = kanamycin resistance, Cm^R = chloramphenicol resistance, Amp^R = ampicillin resistance.

The pZE21s1-*cat* plasmid was introduced into E. coli DH5αPro cells by itself (99, 116), with a plasmid containing *bla* (pZA1), or with a plasmid containing *cat* (pZA3) (Figure 16). GFP output in the presence of *cat* was approximately twice the output obtained in the presence of *bla* or without any plasmid at all (Figure 17). Thus, pZE21s1-*cat* is able to detect the presence of a specific mRNA species encoding an antibiotic-resistance gene *in vivo* and can transduce the detection signal through a simple reporter effector component, GFP.

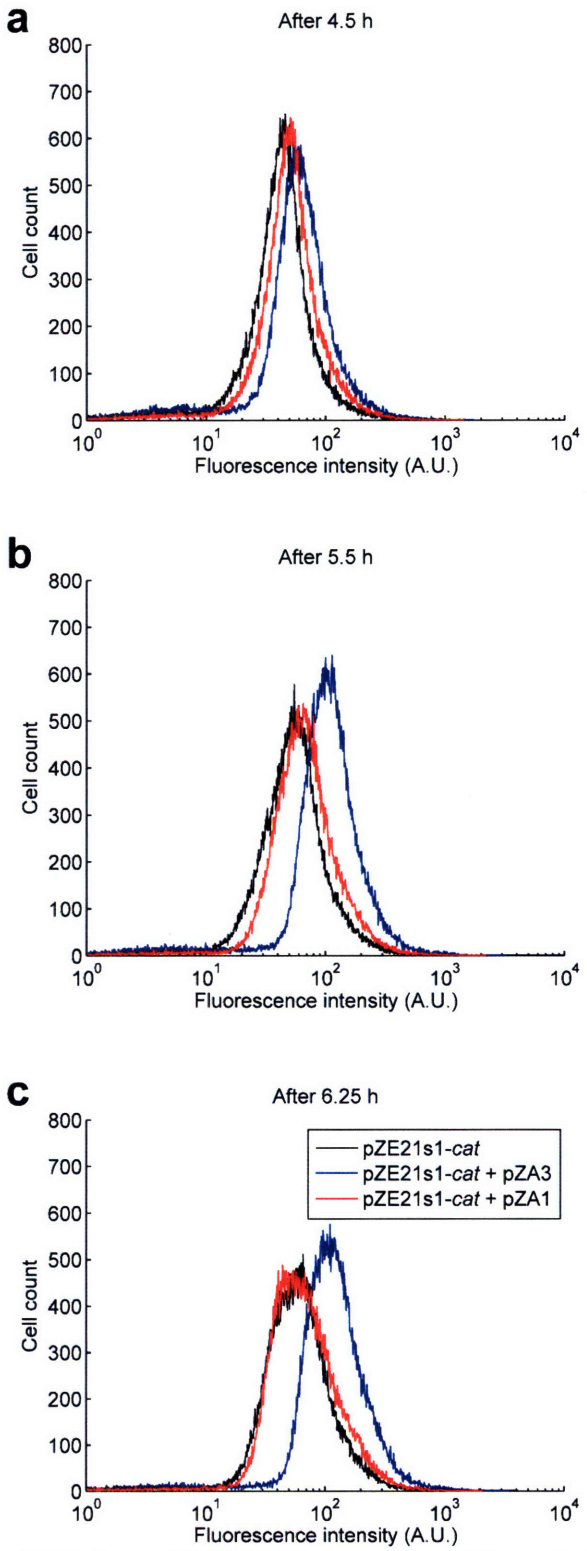

Figure 17. Testing DH5αPro + pZE21s1-*cat* with 1:100 dilutions of overnight stocks in 3 mL LB + kanamycin (30 μg/mL) at 37˚C with 0.1% arabinose and 30 ng/mL aTc. Co-inoculation with pZA3, a *cat*-expressing plasmid, yields an approximately two-fold increase in fluorescence compared with no plasmid or pZA1, a *bla*-expressing plasmid. These results demonstrate that pZE21s1-*cat* functions as a selective mRNA sensor. **(a)** After 4.5 hours of growth. **(b)** After 5.5 hours of growth. **(c)** After 6.25 hours of growth.

4.2.2 Design 2: pTAKs2-*cat* and pTAKs2-*kan*

The second RNA sensor design utilizes the pTAK series of plasmids described in Ref. (117) in which the Lac repressor inhibits expression of GFP by the Ptrc-2 promoter (Figure 18). Antisense RNA targeted towards antibiotic-resistance gene targets such as *cat* or the kanamycin resistance gene (*kan*) are cloned into the untranslated region upstream of the ribosome binding sequence (RBS) for the *lacI* gene (pTAKs2-*cat* and pTAKs2-*kan*, respectively). In this design, PT7 is not used to avoid possible premature termination of the nascent asRNA-*lacI* RNA transcript due to the inverted repeats in the PT7 structure (114). In the absence of the target mRNA, the Lac repressor should repress GFP expression. However, in the presence of the target mRNA, the antisense portion should bind to the target mRNA and cause blocked translation or mRNA degradation of *lacI*, leading to derepression of *gfp*.

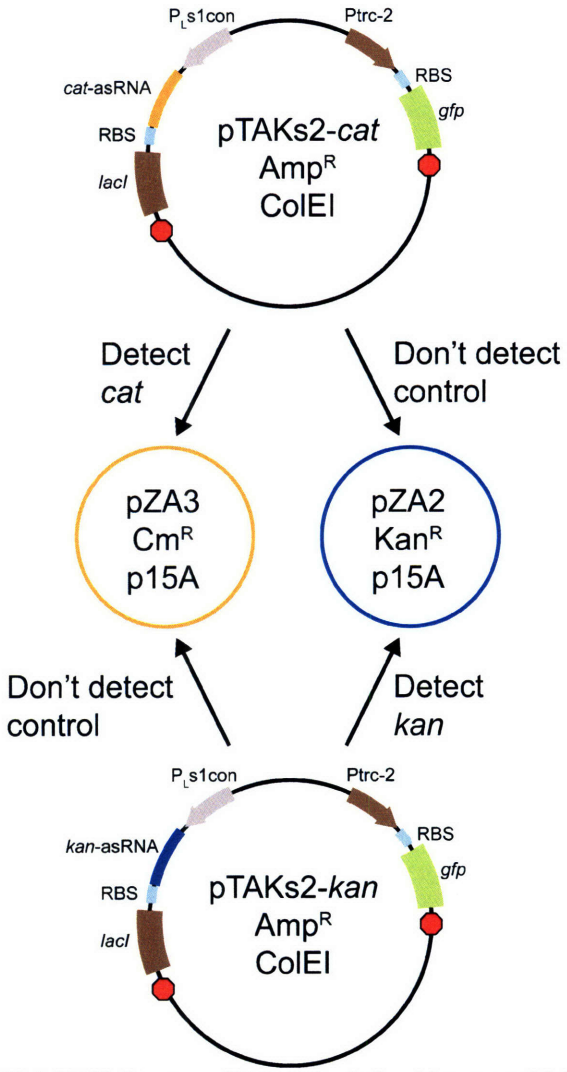

Figure 18. RNA sensor design #2 (pTAKs2-*cat* or pTAKs2-*kan*) should express high levels of *lacI* in the absence of a target-containing plasmid leading to low GFP output. In the presence of a target-containing plasmid, the target mRNA should bind to the asRNA upstream of the *lacI* RBS, leading to blocked translation or mRNA degradation of *lacI* and thus higher GFP output.

The second RNA sensor design shown in Figure 18 was realized by cloning asRNA fragments in between the BspEI and EagI restriction sites in pTAK132 from Ref. (117). The *cI857* gene in pTAK132 was removed by restriction digest in order to obtain continuous output behavior rather than discontinuous switch behavior. Testing was performed by co-transforming sensor-reporter plasmids (pTAKs2-*cat* and pTAKs2-*kan*) with *cat*- or *kan*-containing plasmids (pZA3 or pZA2, respectively) (Figure 18). The pTAKs2-*cat* construct did not appear to discriminate between *cat* or *kan* transcripts and has high levels of GFP expression in general,

suggesting that the asRNA construct in the 5'-untranslated region of the *lacI* gene drastically reduces *lacI* expression and thus does not function appropriately as an RNA sensor (data not shown). This design may not function properly due to the general inefficiency of asRNA in bacteria, especially without the PT7 construct.

4.3 Future Work

4.3.1 Design 3: pTAKs3-*cat*

In addition to the two aforementioned designs, a third RNA sensor design could utilize the pTAK series of plasmids described in Ref. (117). Instead of cloning the antisense RNA for the target RNA into the upstream region of *lacI*, the PT7-*cat*-asRNA construct could be placed just downstream of the *lacI* gene to create pTAKs3-*cat* (Figure 19). This design should only work if the primary mode of the PT7 construct's antisense RNA action is through RNA degradation since it relies on *lacI*-PT7-*cat*-asRNA binding to *cat* mRNA to trigger degradation of the *lacI*-PT7-*cat*-asRNA RNA (114). Reduction of the levels of the Lac repressor should increase GFP output.

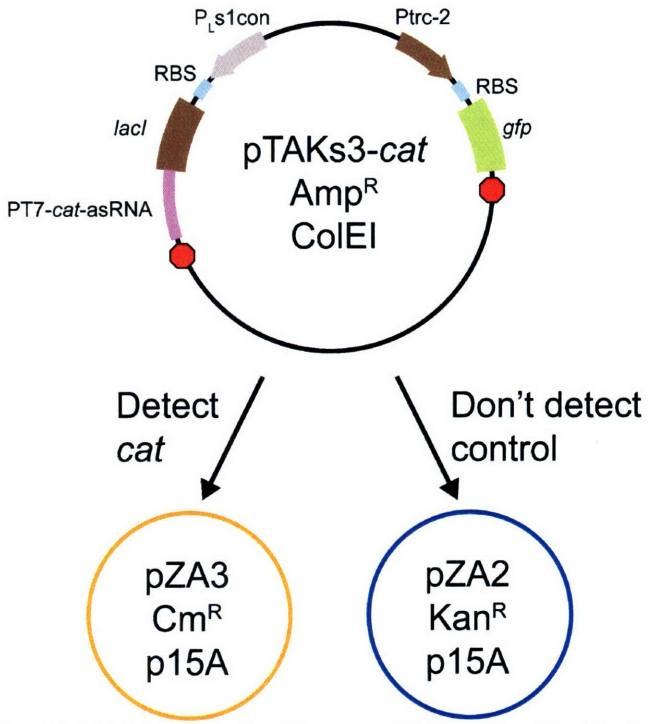

Figure 19. RNA sensor design #3 (pTAKs3-*cat*) should express high levels of *lacI* in the absence of a target-containing plasmid leading to low GFP output. In the presence of a target-containing plasmid, the target mRNA should bind to the PT7-asRNA, leading to mRNA degradation of *lacI* and thus higher GFP output.

The third RNA sensor design shown in Figure 19 can be realized by cloning PT7-asRNA fragments into the AscI site in pTAK132 from Ref. (117). The *cI857* gene in pTAK132 can be removed by restriction digest in order to obtain a continuous output behavior rather than discontinuous switch behavior. The sensor-reporter plasmid (pTAKs3-*cat*) can be co-transformed with *cat*- or *kan*-containing plasmids (pZA3 or pZA2, respectively) for testing (Figure 19).

4.3.2 Autoregulated Synthetic Gene Circuits for Suppressing Horizontal Transmission of Antibiotic Resistance

Antibiotics can mobilize antibiotic-resistance genes by causing cleavage of repressor proteins which normally suppress horizontal transmission in antibiotic-resistance operons (77). A synthetic gene circuit designed to have the repressor suppress its own production in an autoregulated negative feedback loops results in repressor overexpression in the presence of

antibiotics, thus reducing horizontal transmission. In the absence of antibiotics or antibiotic-resistance opersons, the circuit remains dormant and avoids imposing evolutionary fitness costs. This system can be used with repressors like SetR, which represses horizontal transmission of integrating conjugative elements conferring resistance to antibiotics such as chloramphenicol, sulphamethoxazole, trimethoprim and streptomycin (77).

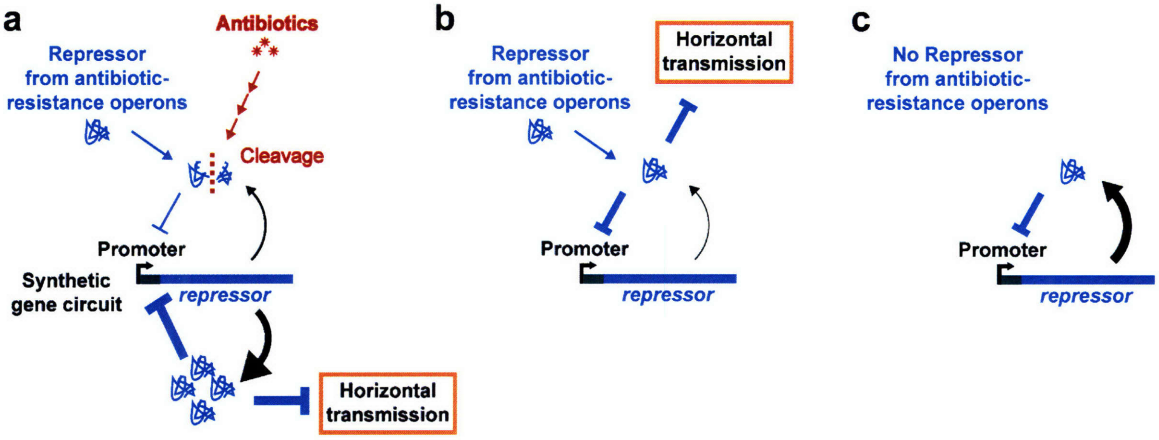

Figure 20. Synthetic gene circuit represses horizontal transmission of antibiotic-resistance genes using an autoregulated negative-feedback loop. **(a)** Antibiotics can cause cleavage of repressors (such as SetR) which suppress horizontal transmission in their normal intact state. Cleavage of repressors from antibiotic-resistance operons in resistant cells results in promoter derepression and subsequent overexpression of repressor from the synthetic gene circuit. The high level of repressor results in the suppression of horizontal transmission, even in the face of antibiotics. In this circuit, the repressor protein serves as both "sensor" and "effector". **(b)** In the absence of antibiotics, repressor produced from antibiotic-resistance operons suppress the synthetic gene circuit and leave it dormant. **(c)** In the absence of antibiotic-resistance operons (in non-resistant cells), the synthetic gene circuit represses itself and therefore exhibits little activity.

4.4 Discussion

Successful *in vivo* sensors for antibiotic-resistance genes could be coupled to a switch to generate threshold-dependent outputs rather than a continuous set of output values. This could be accomplished by replacing the *gfp* gene in pZE21s1-*cat* with *lacI* and integrating the system with previously-designed switches (117). If the output were a toxic gene, the entire sensor-kill system could be introduced into a population of cells with phage, transposons, or conjugative plasmids to allow the selective-reduction of antibiotic resistance in a population. The toxic gene could be further repressed in the absence of the target gene by placing it under *cis*-repressed

control and having a *trans*-activating RNA expressed in the presence of the target gene (116). This method should exhibit less selective pressure on cells especially compared with antibiotics that kill indiscriminately and may be a useful tool in trying to revert populations to susceptibility. One could imagine "vaccinating" a population of bacteria against acquiring antibiotic resistance genes by construct a sensor-kill system on a mobile genetic element that can spread throughout bacterial populations. Such a system could be used to limit the development and spread of antibiotic resistance in livestock in response to antibiotic use in agricultural settings.

Selective killing of bacteria is important to avoid rapid evolution towards antibiotic resistance and bacterial overgrowth diseases such as *Clostridium difficile*-associated disease. Finally, if such an RNA sensor can work in bacteria, where antisense RNAs are inherently inefficient due to transcription-translation coupling (114), an analogous system could be built in eukaryotic cells where effective RNAi mechanisms are present. The general concept of an RNA sensor could be applied to creating selective cancer treatments or killing cells that carry the Human Immunodeficiency Virus.

5 CONCLUSIONS

The synthetic antibacterial strategies I have described above are inexpensive solutions for the looming threat of antibiotic-resistant bacteria and difficult-to-eradicate bacterial biofilms. They are economical and straightforward to design and produce because they utilize rational, nucleic-acid-based technologies. As DNA synthesis and sequencing technologies continue to advance, the appeal of these antibacterial strategies to the biotechnology and pharmaceutical industries should increase dramatically due to their cost-effectiveness, flexibility, and effectiveness as antimicrobial strategies. Since these novel strategies may not be immediately adopted by today's risk-averse medical environment, they can be first applied in industrial and agricultural settings to eliminate troublesome bacteria and reduce the incidence of community-acquired antibiotic resistance. Eventually, the use of these solutions in clinical medicine will help alleviate the monetary and personal costs of antibiotic resistance and difficult-to-eradicate biofilms and improve the general health of human population. Since bacteria continue to evolve mechanisms to defend themselves against modern-day drugs, it is imperative that society stay ahead in the antimicrobial arms race by adopting novel antimicrobial strategies. These solutions should be useful additions to society's arsenal of antimicrobial treatments.

6 REFERENCES

1. Wise, R (2004) *J Antimicrob Chemother* 54: 306-310.

2. Xavier, JB, Picioreanu, C, Rani, SA, van Loosdrecht, MCM & Stewart, PS (2005) *Microbiology* 151: 3817-3832.

3. Davey, ME & O'Toole, GA (2000) *Microbiol Mol Biol Rev* 64: 847-867.

4. Parsek, MR & Singh, PK (2003) *Annual Review of Microbiology* 57: 677-701.

5. Stewart, PS & Costerton, JW (2001) *Lancet* 358: 135-138.

6. Hoffman, LR, D'Argenio, DA, MacCoss, MJ, Zhang, Z, Jones, RA & Miller, SI (2005) *Nature* 436: 1171-1175.

7. Alekshun, MN & Levy, SB (2007) *Cell* 128: 1037-1050.

8. Shah, D, Zhang, Z, Khodursky, A, Kaldalu, N, Kurg, K & Lewis, K (2006) *BMC Microbiol* 6: 53.

9. Hall-Stoodley, L, Costerton, JW & Stoodley, P (2004) *Nat Rev Microbiol* 2: 95-108.

10. Levin, BR & Bonten, MJM (2004) *Proc Natl Acad Sci U S A* 101: 13101-13102.

11. Projan, S (2004) *Nat Biotechnol* 22: 167-168.

12. Schoolnik, GK, Summers, WC & Watson, JD (2004) *Nat Biotechnol* 22: 505-506; author reply 506-507.

13. Vandenesch, F, Naimi, T, Enright, MC, Lina, G, Nimmo, GR, Heffernan, H, Liassine, N, Bes, M, Greenland, T, Reverdy, M-E & Etienne, J (2003) *Emerg Infect Dis* 9: 978-984.

14. (1999) *JAMA* 282: 1123-1125.

15. Hall, BG (2004) *Nat Rev Microbiol* 2: 430-435.

16. Loose, C, Jensen, K, Rigoutsos, I & Stephanopoulos, G (2006) *Nature* 443: 867-869.

17. Kolter, R & Greenberg, EP (2006) *Nature* 441: 300-302.

18. Costerton, JW, Stewart, PS & Greenberg, EP (1999) *Science* 284: 1318-1322.

19. Morens, DM, Folkers, GK & Fauci, AS (2004) *Nature* 430: 242-249.

20. Salyers, AA, Gupta, A & Wang, Y (2004) *Trends Microbiol* 12: 412-416.

21. Wiuff, C, Zappala, RM, Regoes, RR, Garner, KN, Baquero, F & Levin, BR (2005) *Antimicrob Agents Chemother* 49: 1483-1494.

22. Lewis, K (2005) *Biochemistry (Mosc)* 70: 267-274.

23. Korch, SB & Hill, TM (2006) *J Bacteriol* 188: 3826-3836.

24. Vázquez-Laslop, N, Lee, H & Neyfakh, AA (2006) *J Bacteriol* 188: 3494-3497.

25. Bergstrom, CT, Lo, M & Lipsitch, M (2004) *Proc Natl Acad Sci U S A* 101: 13285-13290.

26. Curtin, JJ & Donlan, RM (2006) *Antimicrob Agents Chemother* 50: 1268-1275.

27. Shuren, J (2006), ed. U.S. Food and Drug Administration, H (Federal Register, Vol. 71, pp. 47729-47732.

28. Merril, CR, Scholl, D & Adhya, SL (2003) *Nat Rev Drug Discov* 2: 489-497.

29. Summers, WC (2001) *Annual Review of Microbiology* 55: 437-451.

30. Merril, CR, Biswas, B, Carlton, R, Jensen, NC, Creed, GJ, Zullo, S & Adhya, S (1996) *Proc Natl Acad Sci U S A* 93: 3188-3192.

31. Hagens, S & Blasi, U (2003) *Lett Appl Microbiol* 37: 318-323.

32. Hagens, S, Habel, AvAU, von Gabain, A & Blasi, U (2004) *Antimicrob Agents Chemother* 48: 3817-3822.

33. Boratynski, J, Syper, D, Weber-Dabrowska, B, Lusiak-Szelachowska, M, Pozniak, G & Gorski, A (2004) *Cell Mol Biol Lett* 9: 253-259.

34. Bartlett, JG (2006) *Ann Intern Med* 145: 758-764.

35. Aslam, S, Hamill, RJ & Musher, DM (2005) *Lancet Infect Dis* 5: 549-557.

36. Endy, D (2005) *Nature* 438: 449-453.

37. Andrianantoandro, E, Basu, S, Karig, DK & Weiss, R (2006) *Mol Syst Biol* 2: 2006.0028.

38. Hasty, J, McMillen, D & Collins, JJ (2002) *Nature* 420: 224-230.

39. Tian, J, Gong, H, Sheng, N, Zhou, X, Gulari, E, Gao, X & Church, G (2004) *Nature* 432: 1050-1054.

40. Ro, D-K, Paradise, EM, Ouellet, M, Fisher, KJ, Newman, KL, Ndungu, JM, Ho, KA, Eachus, RA, Ham, TS, Kirby, J, Chang, MCY, Withers, ST, Shiba, Y, Sarpong, R & Keasling, JD (2006) *Nature* 440: 940-943.

41. Anderson, JC, Clarke, EJ, Arkin, AP & Voigt, CA (2006) *J Mol Biol* 355: 619-627.

42. Lu, TK & Collins, JJ (2007) *Proc Natl Acad Sci U S A* 104: 11197-11202.

43. Costerton, JW, Lewandowski, Z, Caldwell, DE, Korber, DR & Lappin-Scott, HM (1995) *Annu Rev Microbiol* 49: 711-745.

44. Merril, CR, Scholl, D & Adhya, SL (2003) *Nat Rev Drug Discov* 2: 489--497.

45. Doolittle, MM, Cooney, JJ & Caldwell, DE (1995) *Can J Microbiol* 41: 12-18.

46. Doolittle, MM, Cooney, JJ & Caldwell, DE (1996) *J Ind Microbiol* 16: 331-341.

47. Corbin, BD, McLean, RJ & Aron, GM (2001) *Can J Microbiol* 47: 680-684.

48. Scholl, D, Adhya, S & Merril, C (2005) *Appl Environ Microbiol* 71: 4872-4874.

49. Itoh, Y, Wang, X, Hinnebusch, BJ, Preston, JF & Romeo, T (2005) *J Bacteriol* 187: 382-387.

50. Whitchurch, CB, Tolker-Nielsen, T, Ragas, PC & Mattick, JS (2002) *Science* 295: 1487.

51. Itoh, Y, Wang, X, Hinnebusch, BJ, Preston, JF & Romeo, T (2005) *J Bacteriol* 187: 382--387.

52. Hughes, KA, Sutherland, IW & Jones, MV (1998) *Microbiology* 144 (Pt 11): 3039--3047.

53. Hughes, KA, Sutherland, IW, Clark, J & Jones, MV (1998) *Journal of Applied Microbiology* 85: 583-590.

54. Hughes, KA, Sutherland, IW & Jones, MV (1998) *Microbiology* 144 (Pt 11): 3039-3047.

55. Chan, LY, Kosuri, S & Endy, D (2005) *Mol Syst Biol* 1: 2005.0018.

56. Itaya, M, Tsuge, K, Koizumi, M & Fujita, K (2005) *Proc Natl Acad Sci U S A* 102: 15971-15976.

57. Dunn, JJ & Studier, FW (1983) *J Mol Biol* 166: 477-535.

58. Studier, FW & Dunn, JJ (1983) *Cold Spring Harb Symp Quant Biol* 47 Pt 2: 999-1007.

59. Ghigo, JM (2001) *Nature* 412: 442-445.

60. Re, SD, Quéré, BL, Ghigo, J-M & Beloin, C (2007) *Appl Environ Microbiol.*

61. Garcia, LR & Molineux, IJ (1995) *J Bacteriol* 177: 4077-4083.

62. Jackson, DW, Suzuki, K, Oakford, L, Simecka, JW, Hart, ME & Romeo, T (2002) *J Bacteriol* 184: 290-301.

63. Studier, FW (1972) *Science* 176: 367-376.

64. Tian, J, Gong, H, Sheng, N, Zhou, X, Gulari, E, Gao, X & Church, G (2004) *Nature* 432: 1050--1054.

65. Baker, D, Church, G, Collins, J, Endy, D, Jacobson, J, Keasling, J, Modrich, P, Smolke, C & Weiss, R (2006) *Sci Am* 294: 44-51.

66. Hickman-Brenner, FW, Stubbs, AD & Farmer, JJ (1991) *J Clin Microbiol* 29: 2817-2823.

67. Wentworth, BB (1963) *Bacteriol Rev* 27: 253-272.

68. Doulatov, S, Hodes, A, Dai, L, Mandhana, N, Liu, M, Deora, R, Simons, RW, Zimmerly, S & Miller, JF (2004) *Nature* 431: 476-481.

69. Liu, M, Deora, R, Doulatov, SR, Gingery, M, Eiserling, FA, Preston, A, Maskell, DJ, Simons, RW, Cotter, PA, Parkhill, J & Miller, JF (2002) *Science* 295: 2091-2094.

70. Datsenko, KA & Wanner, BL (2000) *Proc Natl Acad Sci U S A* 97: 6640-6645.

71. Ceri, H, Olson, ME, Stremick, C, Read, RR, Morck, D & Buret, A (1999) *J Clin Microbiol* 37: 1771-1776.

72. Walsh, C (2003) *Nat Rev Microbiol* 1: 65-70.

73. Balaban, NQ, Merrin, J, Chait, R, Kowalik, L & Leibler, S (2004) *Science* 305: 1622-1625.

74. Lewis, K (2007) *Nat Rev Microbiol* 5: 48-56.

75. Avery, SV (2006) *Nat Rev Microbiol* 4: 577-587.

76. Chang, S, Sievert, DM, Hageman, JC, Boulton, ML, Tenover, FC, Downes, FP, Shah, S, Rudrik, JT, Pupp, GR, Brown, WJ, Cardo, D, Fridkin, SK & Vancomycin-Resistant Staphylococcus aureus Investigative Team (2003) *N Engl J Med* 348: 1342-1347.

77. Beaber, JW, Hochhut, B & Waldor, MK (2004) *Nature* 427: 72-74.

78. Ubeda, C, Maiques, E, Knecht, E, Lasa, I, Novick, RP & Penadés, JR (2005) *Mol Microbiol* 56: 836-844.

79. Klevens, RM, Morrison, MA, Nadle, J, Petit, S, Gershman, K, Ray, S, Harrison, LH, Lynfield, R, Dumyati, G, Townes, JM, Craig, AS, Zell, ER, Fosheim, GE, McDougal, LK, Carey, RB, Fridkin, SK & Active Bacterial Core Surveillance MRSA Investigators (2007) *JAMA* 298: 1763-1771.

80. Brown, EM & Nathwani, D (2005) *J Antimicrob Chemother* 55: 6-9.

81. Soulsby, EJ (2005) *BMJ* 331: 1219-1220.

82. Soulsby, L (2007) *J Antimicrob Chemother* 60 Suppl 1: i77-i78.

83. Wang, J, Soisson, SM, Young, K, Shoop, W, Kodali, S, Galgoci, A, Painter, R, Parthasarathy, G, Tang, YS, Cummings, R, Ha, S, Dorso, K, Motyl, M, Jayasuriya, H, Ondeyka, J, Herath, K, Zhang, C, Hernandez, L, Allocco, J, Basilio, A, Tormo, JR, Genilloud, O, Vicente, F, Pelaez, F, Colwell, L, Lee, SH, Michael, B, Felcetto, T, Gill, C, Silver, LL, Hermes, JD, Bartizal, K, Barrett, J, Schmatz, D, Becker, JW, Cully, D & Singh, SB (2006) *Nature* 441: 358-361.

84. Westwater, C, Kasman, LM, Schofield, DA, Werner, PA, Dolan, JW, Schmidt, MG & Norris, JS (2003) *Antimicrob Agents Chemother* 47: 1301-1307.

85. Heitman, J, Fulford, W & Model, P (1989) *Gene* 85: 193-197.

86. Brüssow, H (2005) *Microbiology* 151: 2133-2140.

87. Bonhoeffer, S, Lipsitch, M & Levin, BR (1997) *Proc Natl Acad Sci U S A* 94: 12106-12111.

88. Chait, R, Craney, A & Kishony, R (2007) *Nature* 446: 668-671.

89. Levy, SB & Marshall, B (2004) *Nat Med* 10: S122-S129.

90. Dwyer, DJ, Kohanski, MA, Hayete, B & Collins, JJ (2007) *Mol Syst Biol* 3: 91.

91. Kohanski, MA, Dwyer, DJ, Hayete, B, Lawrence, CA & Collins, JJ (2007) *Cell* 130: 797-810.

92. Cottarel, G & Wierzbowski, J (2007) *Trends Biotechnol.*

93. Miller, C, Thomsen, LE, Gaggero, C, Mosseri, R, Ingmer, H & Cohen, SN (2004) *Science* 305: 1629-1631.

94. Lewin, CS, Howard, BM, Ratcliffe, NT & Smith, JT (1989) *J Med Microbiol* 29: 139-144.

95. Little, JW & Harper, JE (1979) *Proc Natl Acad Sci U S A* 76: 6147-6151.

96. Yanisch-Perron, C, Vieira, J & Messing, J (1985) *Gene* 33: 103-119.

97. Hagens, S, Habel, A & Bläsi, U (2006) *Microb Drug Resist* 12: 164-168.

98. Walker, GC (1984) *Microbiol Rev* 48: 60-93.

99. Lutz, R & Bujard, H (1997) *Nucleic Acids Res* 25: 1203-1210.

100. Little, JW, Edmiston, SH, Pacelli, LZ & Mount, DW (1980) *Proc Natl Acad Sci U S A* 77: 3225-3229.

101. Martinez, JL & Baquero, F (2000) *Antimicrob Agents Chemother* 44: 1771-1777.

102. Hidalgo, E, Ding, H & Demple, B (1997) *Cell* 88: 121-129.

103. Hidalgo, E, Ding, H & Demple, B (1997) *Trends Biochem Sci* 22: 207-210.

104. Chander, M, Raducha-Grace, L & Demple, B (2003) *J Bacteriol* 185: 2441-2450.

105. Blanchard, JL, Wholey, W-Y, Conlon, EM & Pomposiello, PJ (2007) *PLoS ONE* 2: e1186.

106. Koutsolioutsou, A, Martins, EA, White, DG, Levy, SB & Demple, B (2001) *Antimicrob Agents Chemother* 45: 38-43.

107. Koutsolioutsou, A, Peña-Llopis, S & Demple, B (2005) *Antimicrob Agents Chemother* 49: 2746-2752.

108. Lewis, K (2001) *Antimicrob Agents Chemother* 45: 999-1007.

109. Lynch, SV, Dixon, L, Benoit, MR, Brodie, EL, Keyhan, M, Hu, P, Ackerley, DF, Andersen, GL & Matin, A (2007) *Antimicrob Agents Chemother* 51: 3650-3658.

110. Hirai, K, Aoyama, H, Irikura, T, Iyobe, S & Mitsuhashi, S (1986) *Antimicrob Agents Chemother* 29: 535-538.

111. Newcomb, J, Carlson, R & Aldrich, S (2007) *Genome Synthesis and Design Futures: Implications for the U.S. Economy* (Bio Economic Research Associates.

112. Kitagawa, M, Ara, T, Arifuzzaman, M, Ioka-Nakamichi, T, Inamoto, E, Toyonaga, H & Mori, H (2005) *DNA Res* 12: 291-299.

113. Okusu, H, Ma, D & Nikaido, H (1996) *J Bacteriol* 178: 306-308.

114. Nakashima, N, Tamura, T & Good, L (2006) *Nucleic Acids Res* 34: e138.

115. Potrykus, J & Wegrzyn, G (2001) *Antimicrob Agents Chemother* 45: 3610-3612.

116. Isaacs, FJ, Dwyer, DJ, Ding, C, Pervouchine, DD, Cantor, CR & Collins, JJ (2004) *Nat Biotechnol* 22: 841-847.

117. Gardner, TS, Cantor, CR & Collins, JJ (2000) *Nature* 403: 339-342.